A Wavelet-based Multifractal Analysis for scalar and vector fields: Application to developped turbulence

Pierre Kestener⋆**, Alain Arneodo**

Laboratoire de Physique, ENS Lyon, France

⋆ *present address: CEA Saclay, DSM/DAPNIA/SEDI, Gif-Sur-Yvette, FRANCE*

Contents

- ☞ Introduction
- ☞ Characterization of multifractal images with the 2D WTMM method
- ☞ Generalizations of the WTMM method $\longrightarrow$ from 2D to 3D

  $\longrightarrow$ from scalar to vector

- Application to developped turbulence (direct numerical simulations)

  3D scalar case : dissipation field and enstrophy field

  3D vector case : velocity field and vorticity field

- Application to galaxy distribution (simulation data)

Fractal Objects : self-similarity

- exact self-similarity :

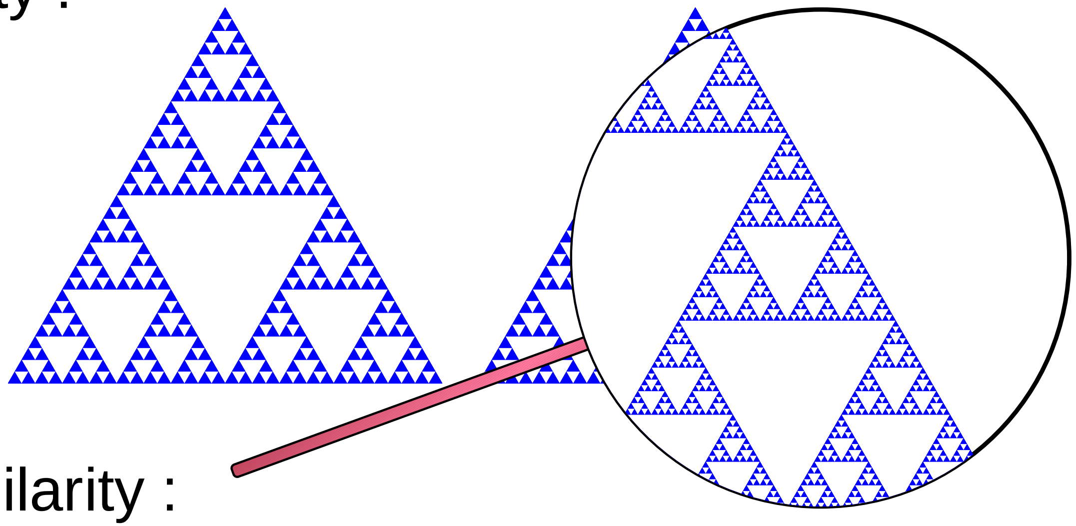

- statistical self-similarity :

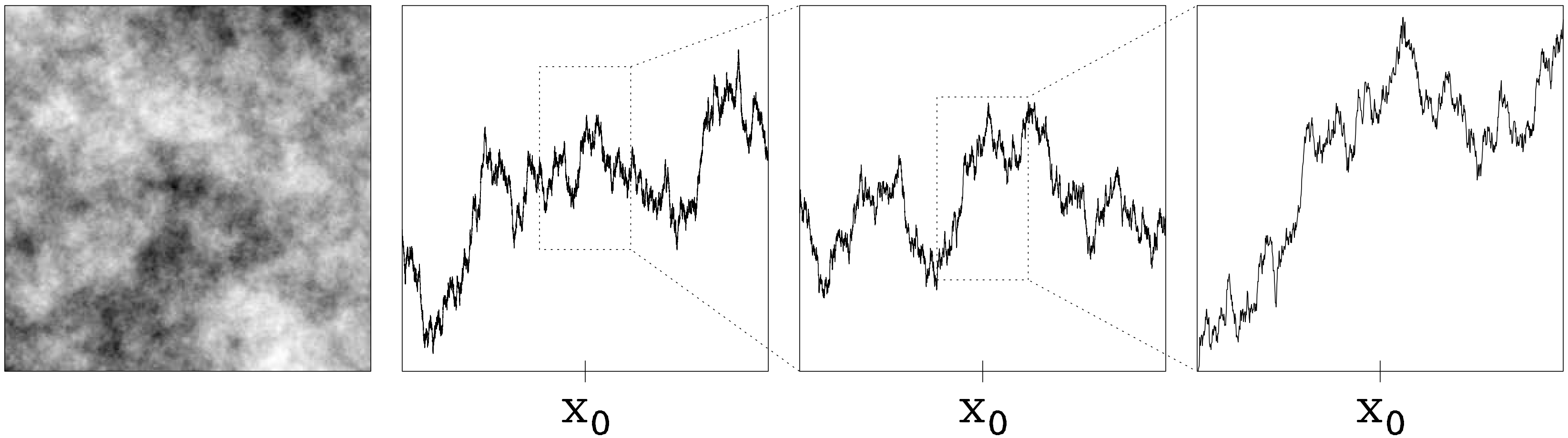

$$\boldsymbol{f}(\mathbf{x}_0 + \boldsymbol{\lambda}\mathbf{u}) - \boldsymbol{f}(\mathbf{x}_0) \sim \boldsymbol{\lambda}^{\boldsymbol{h}(\mathbf{x}_0)}\left(\boldsymbol{f}(\mathbf{x}_0 + \mathbf{u}) - \boldsymbol{f}(\mathbf{x}_0)\right)$$

Self-similarity and Wavelet Transform

- **<u>Wavelet Transform :</u>** **a mathematical microscope to study fractal objects self-similarity properties**

$$T_\psi[f](a,b) = < f, \psi_{a,b} > = \frac{1}{\sqrt{a}} \int_{-\infty}^{+\infty} dx\, f(x) \psi^*(\frac{x-b}{a})$$

- **local self-similarity (Hölder exponent) can be seen in the wavelet transform coefficients under scaling laws (Jaffard, Mallat et coll., Holschneider and Tchamitchian) :**

$$T_\psi[f](a, x_0) \sim a^{h(x_0)+\frac{1}{2}}, \quad a \longrightarrow 0^+$$

- **<u>statistical description of self-similarity :</u>**
  WTMM method (Wavelet Transform Modulus Maxima) by Muzy, Bacry, Arnéodo (1993) for multifractal signals.

- **many applications in bioinformatics (DNA Sequences), in turbulence, in finance, in geophysics,...**

classical multifractal formalism comes from turbulence

- **The Navier-Stokes equations:**

$$\partial_t \mathbf{u} + \mathbf{u}.\nabla\ \mathbf{u} = -\frac{1}{\rho}\nabla p + \mathbf{f} + \nu \mathbf{\Delta u}, \qquad +\nabla.\mathbf{u} = 0 + BC + CI$$

- **turbulent regime :** $||\mathbf{u}.\nabla\ \mathbf{u}|| >> ||\nu\mathbf{\Delta u}||$
- **signal highly disorganized and structures at all scales, unpredictable as for details**

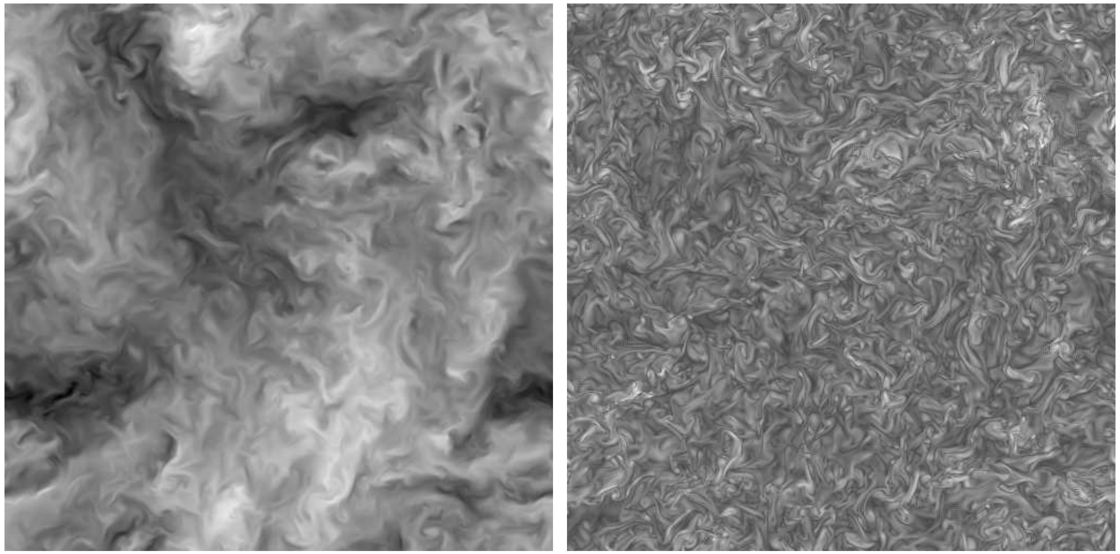

☞ **Statistical tools required**

Multifractal description of intermittency in turbulence

Multifractal description of intermittency in turbulence

- classical multifractal formalism comes from turbulence
  - ☞ multifractal model for velocity : longitudinal structure functions based on (1D) velocity increments :

$$S_p(l) \;=\; <(\mathbf{e}.\delta\mathbf{v}(\mathbf{r}, l\mathbf{e}))^p> \;\sim\; l^{\zeta_p}, \qquad p > 0$$

  - ☞ multifractal model for (1D *surrogate*) dissipation : RSH hypothesis

$$S_p(l) \;\sim\; <\varepsilon_l^{p/3}> l^{p/3} \;\sim\; l^{\tau_\varepsilon(p/3)+p/3}.$$

    Measure of the spectra $\tau_\varepsilon(p)$ and $f(\alpha)$ with the box-counting method.

- multifractal formalism based on WT (WTMM method) for regularity analysis of functions, measures and distributions.

  - ☞ generalization of the WTMM method 1D/2D$\longrightarrow$3D
  - ☞ generalization to multidimensional vector fields. First application to velocity and vorticity fields from numerical turbulent flows.

2D WTMM Methodology : PhD work of N. Decoster

2D data : I

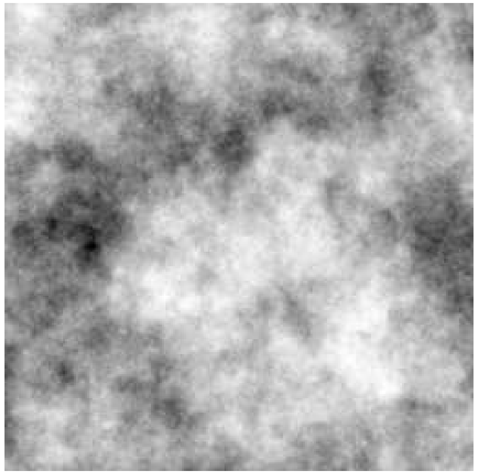

Smoothing scale a

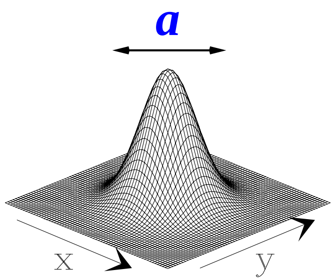

Gradient ∇

$$\left[\frac{\partial}{\partial x}, \frac{\partial}{\partial y}\right]$$

Wavelet Transform

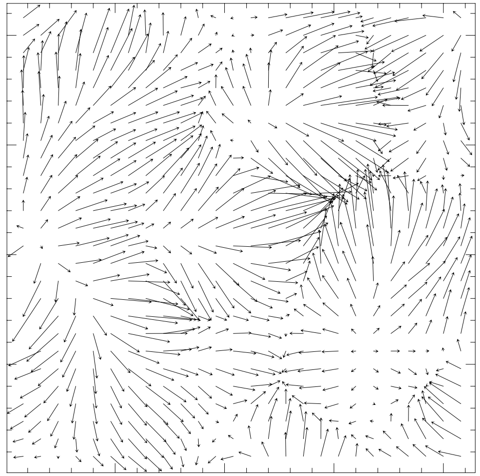

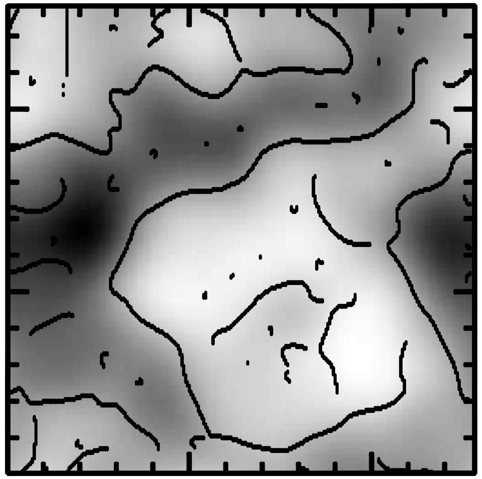

$$\mathbf{T}_{\psi}(\mathbf{r}, a) = \begin{pmatrix} I * \dfrac{\partial \phi_a}{\partial x}(\mathbf{r}) \\ I * \dfrac{\partial \phi_a}{\partial y}(\mathbf{r}) \end{pmatrix}$$

$$\mathbf{T}_{\psi}(\mathbf{r}, a) = \boldsymbol{\nabla}(I * \phi_a)(\mathbf{r}) = (\mathcal{M}_{\psi}(\mathbf{r}, a), \mathcal{A}_{\psi}(\mathbf{r}, a))$$

WTMM Methodology : Skeleton

WTMM Chains

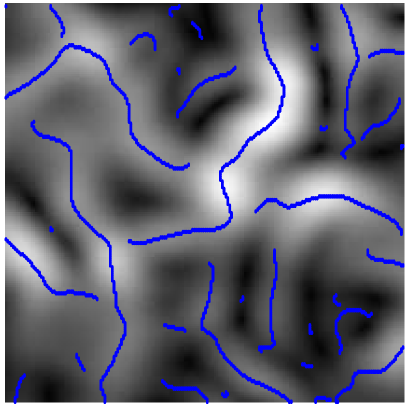

WTMMM

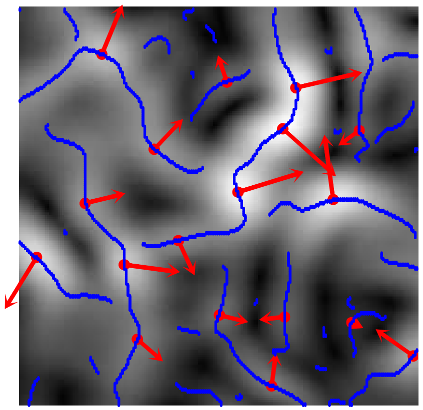

WTMM Chains at 3 different scales

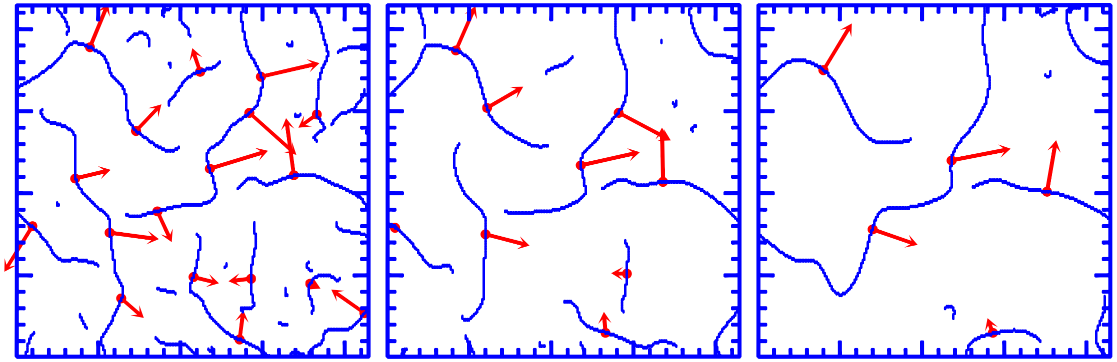

WTMMM linking : WT skeleton

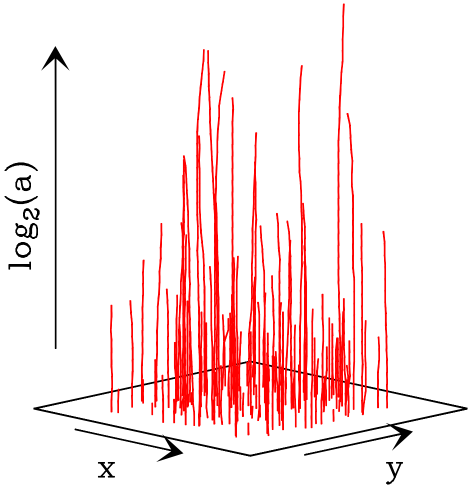

Local roughness characterization : Hölder exponent

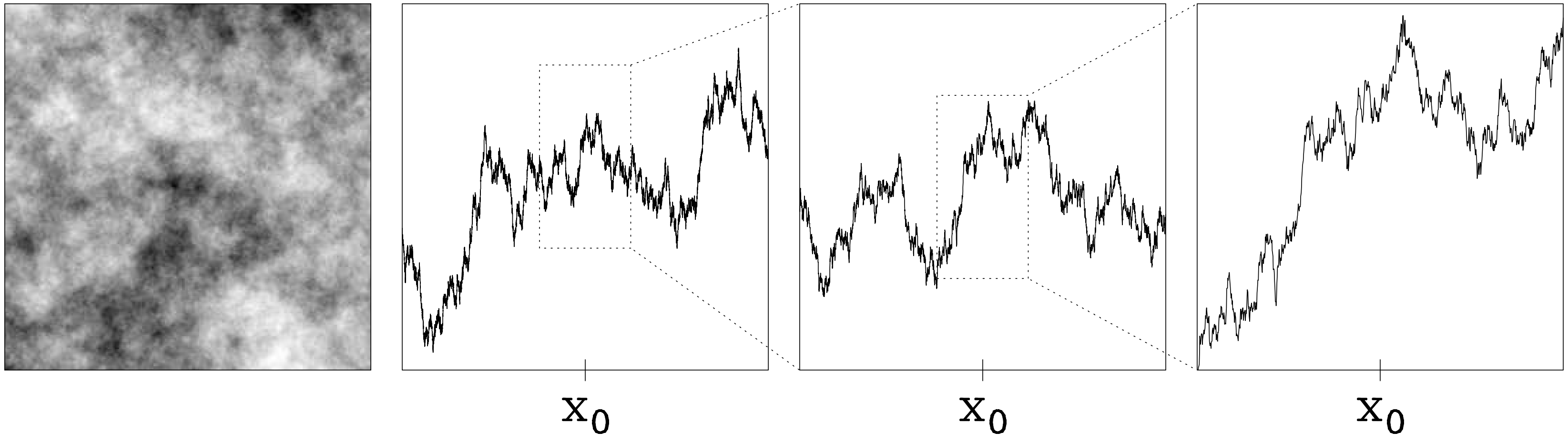

$$f(\mathbf{x_0} + \lambda \mathbf{u}) - f(\mathbf{x_0}) \sim \lambda^{h(\mathbf{x_0})} \left(f(\mathbf{x_0} + \mathbf{u}) - f(\mathbf{x_0}) \right)$$

- **Monofractal Image**
- **Multifractal Image**

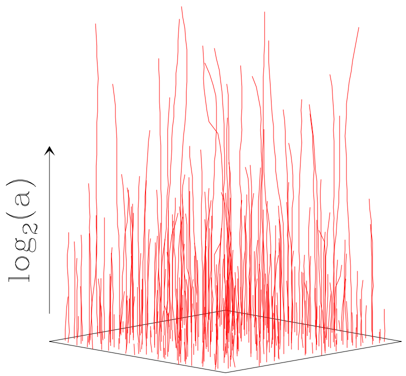

$\mathcal{M} \sim a^{h}$,

single h

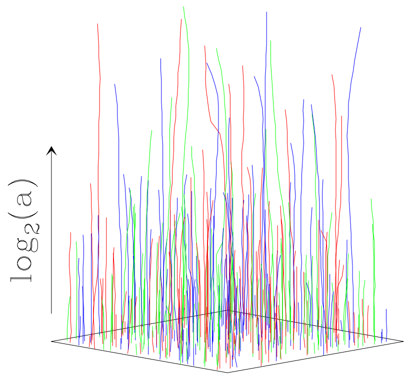

$\mathcal{M} \sim a^{h}, a^{h}, a^{h}$,

$h \in [h_{\min}, h_{\max}]$

WTMM Method : multifractal formalism

Singularity spectrum :

$$\boldsymbol{D}(\boldsymbol{h}) = d_H\{\mathrm{r} \in R^d, h(\mathrm{r}) = h\}$$

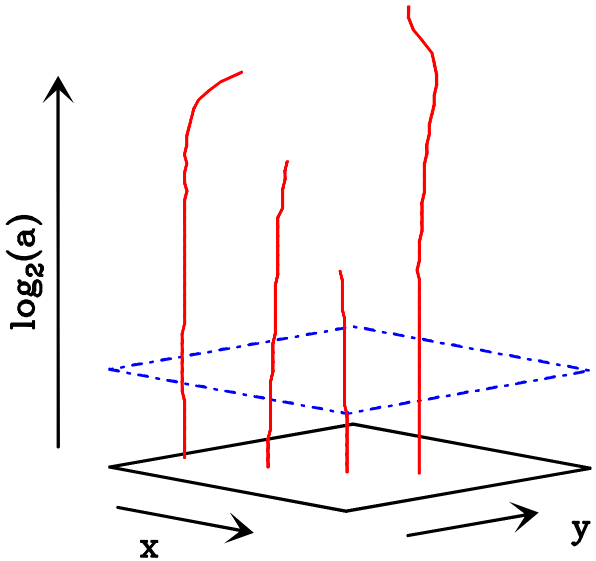

Legendre transform :

$$D(h) = \min_q \Big(qh - \tau(q)\Big)$$

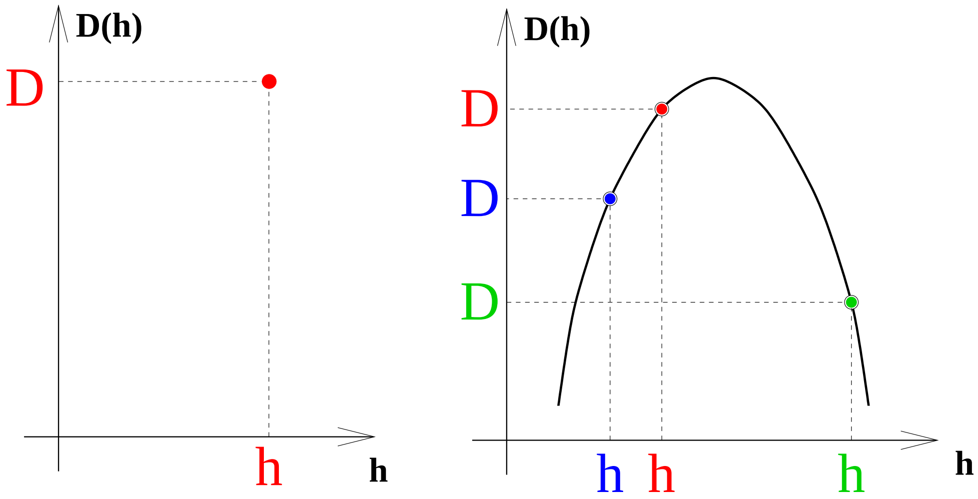

Analogy statistical physics : compute partition functions

$$\mathcal{Z}(q,a) = \sum_{\mathcal{L}(a)} \left(\mathcal{M}_\psi(\mathrm{r},a)\right)^q \sim a^{\tau(q)}$$

WTMM Method : multifractal formalism

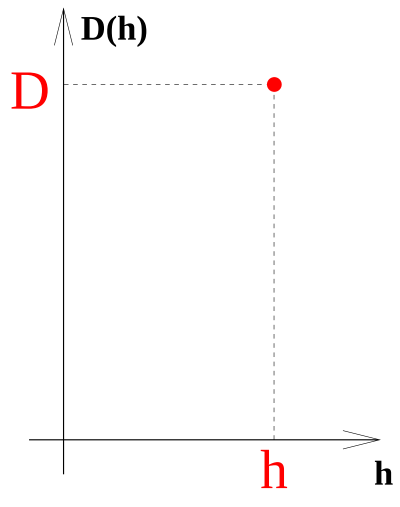

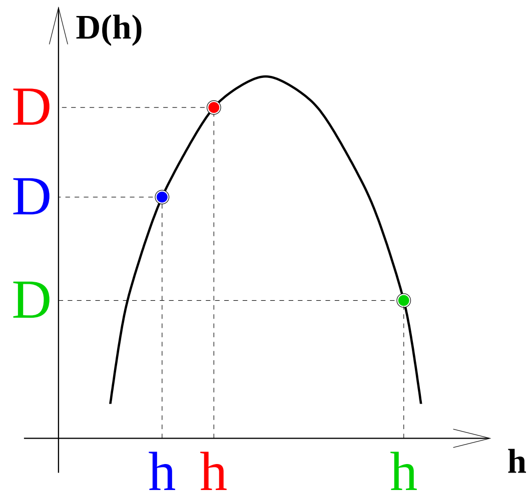

Singularity spectrum :

$$D(h) = d_H\{\mathrm{r} \in R^d, h(\mathrm{r}) = h\}$$

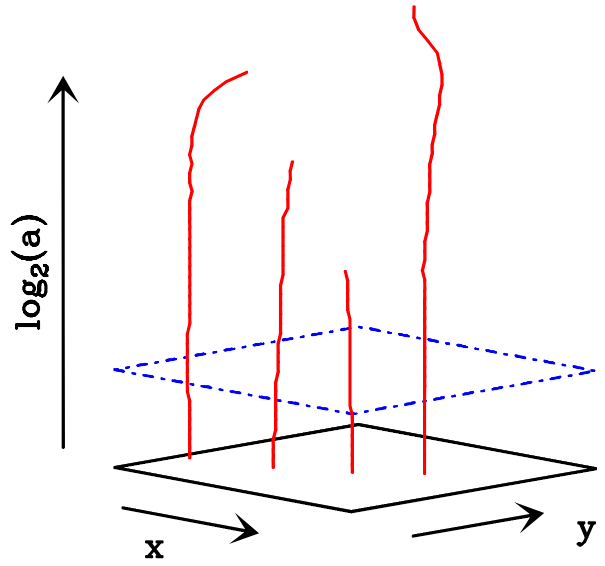

Analogy statistical physics : compute **partition functions**

$$\mathcal{Z}(q,a) = \sum_{\mathcal{L}(a)} \left(\mathcal{M}_\psi(\mathrm{r},a)\right)^q \sim a^{\tau(q)}$$

$$\mathcal{H}(q,a) = \sum_{\mathcal{L}(a)} \ln|\mathcal{M}_\psi(\mathrm{r},a)|\, \mathcal{W}_\psi(\mathrm{r},a) \sim a^{h(q)}$$

$$\mathcal{D}(q,a) = \sum_{\mathcal{L}(a)} \ln|\mathcal{W}_\psi(\mathrm{r},a)|\, \mathcal{W}_\psi(\mathrm{r},a) \sim a^{D(q)}$$

Legendre transform :

$$D(h) = \min_q\left(qh - \tau(q)\right)$$

Application to synthetic **monofractal** surfaces

fractional Brownian surfaces : $B_H(\mathrm{r})$

- $H < 0.5$: anti-correlated increments
- $H = 0.5$: non-correlated increments
- $H > 0.5$: correlated increments

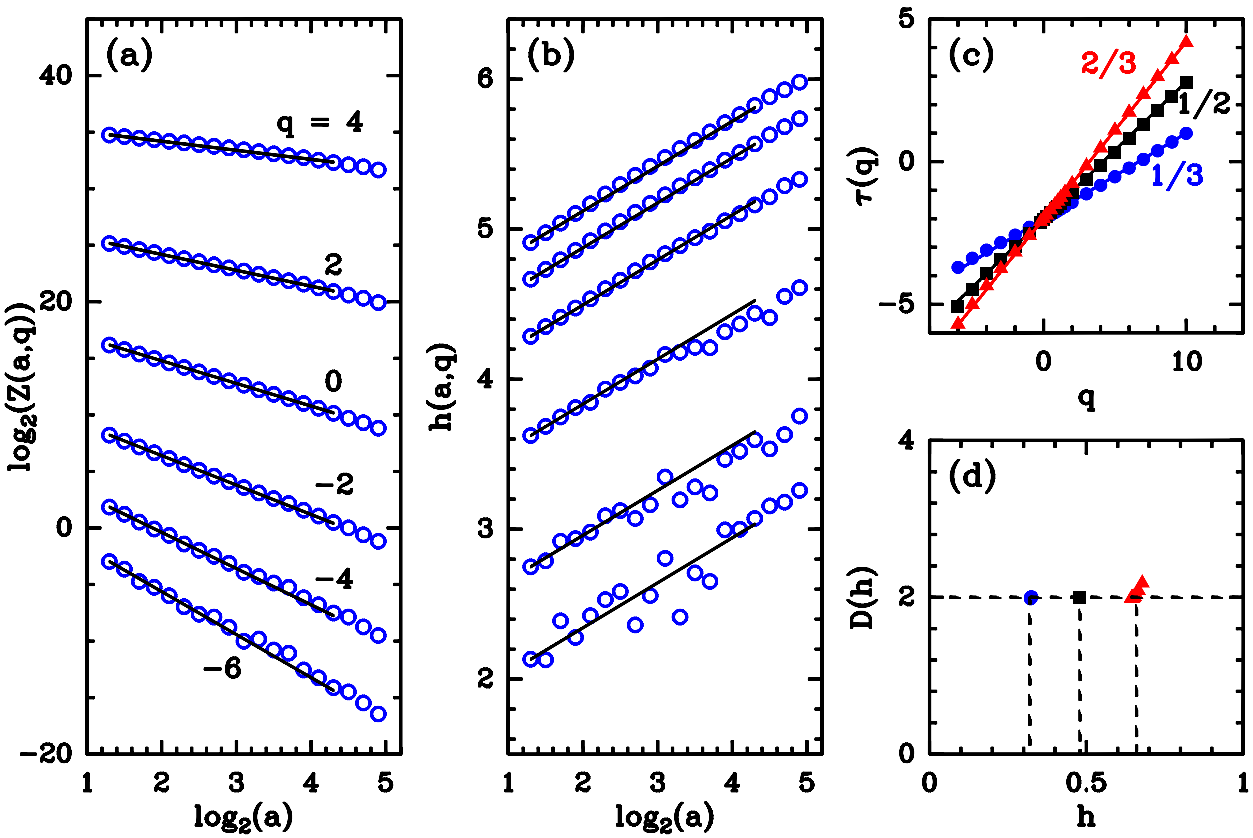

H=1/3

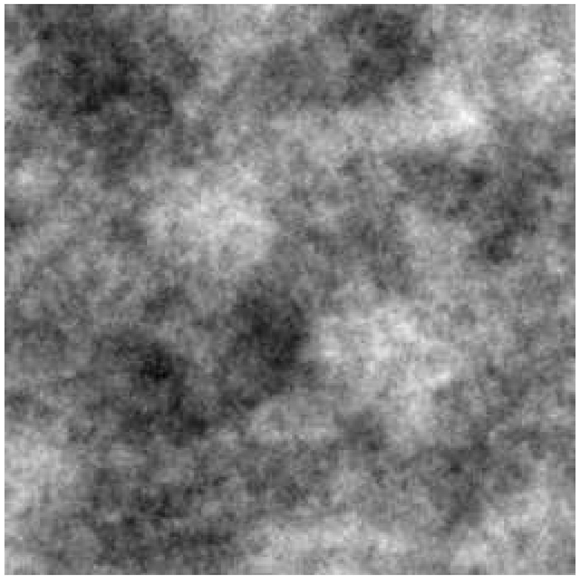

Theoretical Predictions :

- $\tau(q)$ is linear :
  $\tau(q) = qH - 2$
- multifractal spectrum is degenerated :
  $D(h = H) = 2$

Application to synthetic multifractal surfaces

FISC **(Fractionally Integrated Singular Cascades)** model

- simple multiplicative model : p-model or multinomial model

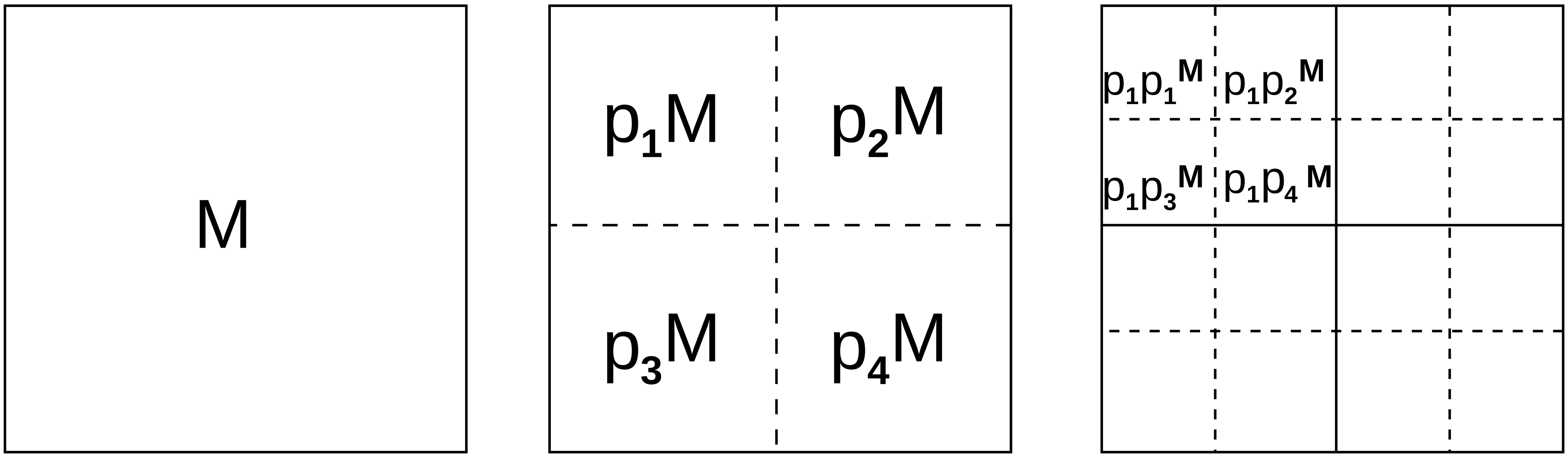

- fractional integration (Fourier domain)
- generalization : p is a random variable with $< p >= 1/4$ (conservative cascading process)

Application to synthetic multifractal surfaces

Multifractal (Fractionally Integrated Singular Cascades) surfaces

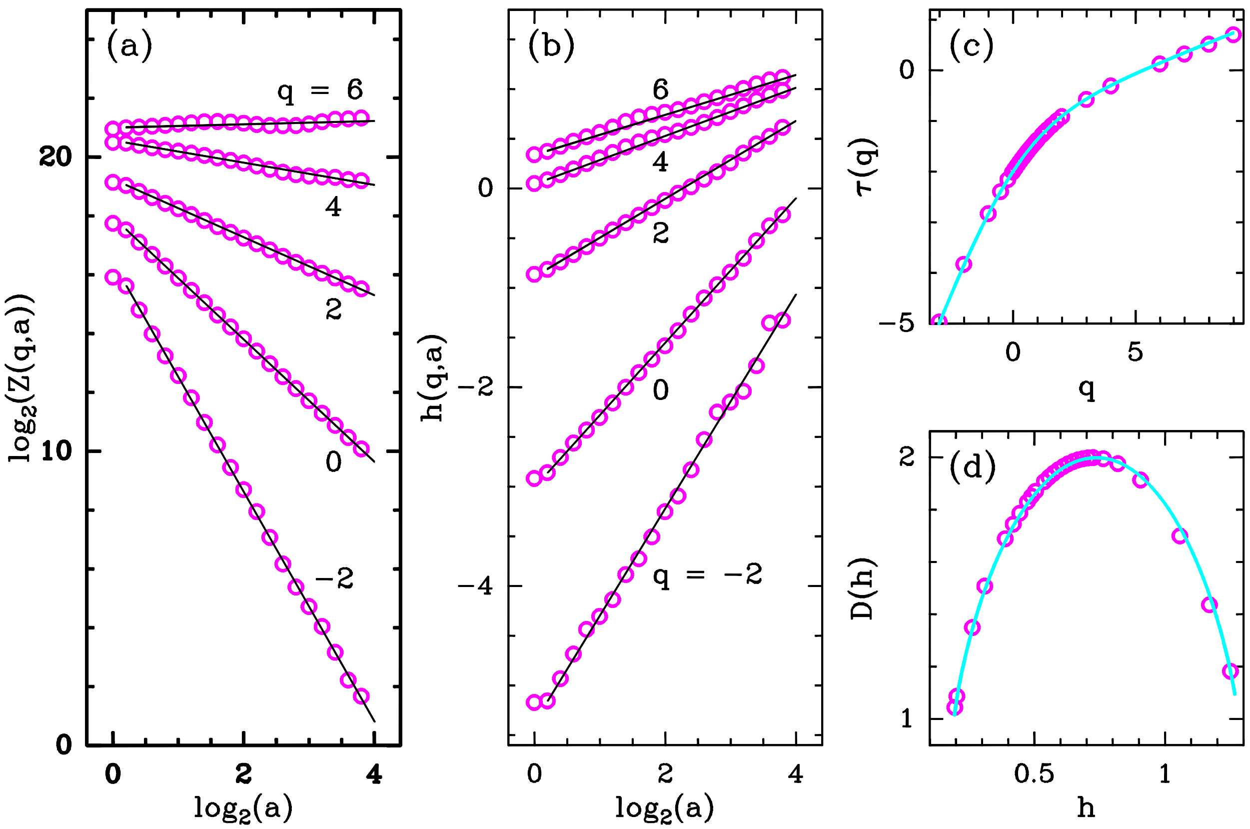

FISC

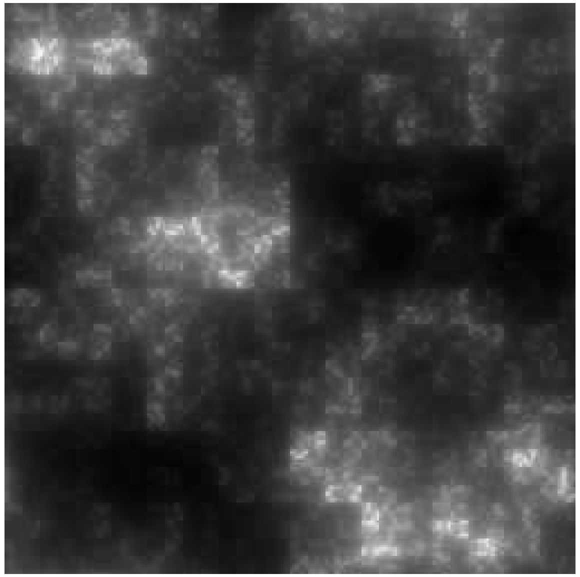

Theoretical predictions :

- $\tau(q)$ is non-linear

$$\tau(q) = -2 - q(1 - H^*) - \log_2({p_1}^q + {p_2}^q)$$

- singularity spectrum is a non-degenerated convex curve

classical multifractal formalism comes from turbulence

- **The Navier-Stokes equations:**

$$\partial_t \mathbf{u} + \mathbf{u}.\nabla\ \mathbf{u} = -\frac{1}{\rho}\nabla p + \mathbf{f} + \nu\boldsymbol{\Delta}\mathbf{u}, \qquad +\nabla.\mathbf{u} = 0 + BC + CI$$

- **turbulent regime :** $||\mathbf{u}.\nabla\ \mathbf{u}|| >> ||\nu\boldsymbol{\Delta}\mathbf{u}||$
- **signal highly disorganized and structures at all scales, unpredictable as for details**

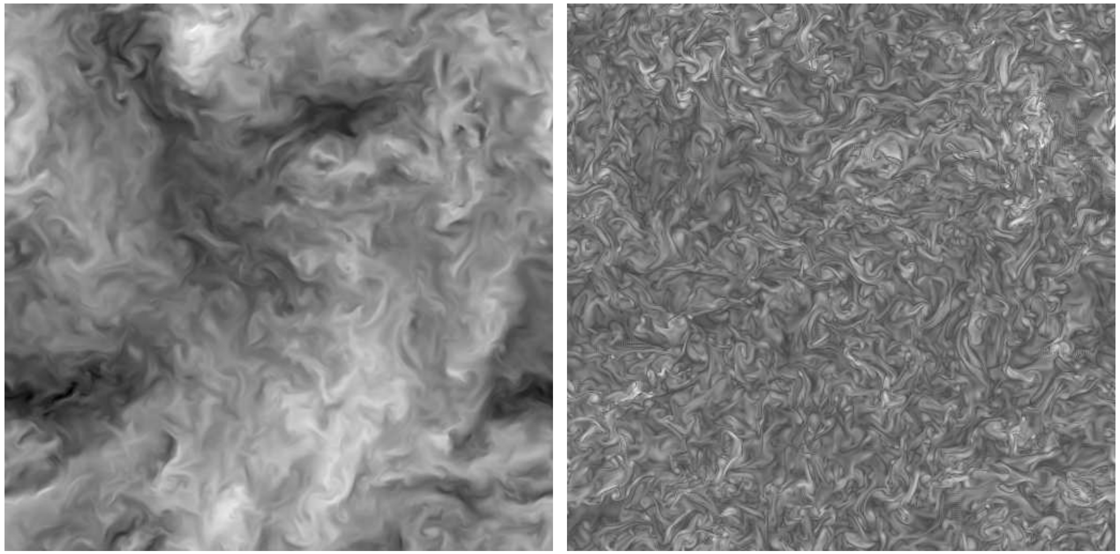

☞ **Statistical tools required**

Multifractal description of intermittency in turbulence

- classical multifractal formalism comes from turbulence
  - ☞ multifractal model for velocity : longitudinal structure functions based on (1D) velocity increments :

$$S_p(l) = < (\mathrm{e}.\delta \mathrm{v}(\mathrm{r}, l\mathrm{e}))^p > \sim l^{\zeta_p}, \qquad p > 0$$

  - ☞ multifractal model for (1D *surrogate*) dissipation : RSH hypothesis

$$S_p(l) \sim < \varepsilon_l^{p/3} > l^{p/3} \sim l^{\tau_\varepsilon(p/3)+p/3}.$$

Measure of the spectra $\tau_\varepsilon(p)$ and $f(\alpha)$ with the box-counting method.

- multifractal formalism based on WT (WTMM method) for regularity analysis of functions, measures and distributions.

> ☞ generalization of the WTMM method 1D/2D⟶3D
>
> ☞ generalization to multidimensional vector fields. First application to velocity and vorticity fields from numerical turbulent flows.

3D scalar WTMM method

3D data

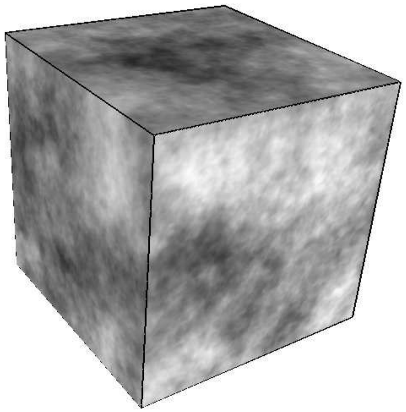

$$\xrightarrow{\text{Smoothing scale } a} \qquad \xrightarrow{\text{Gradient } \nabla}$$

$$\underbrace{{\color{red}\phi_a} \qquad \left[\frac{\partial}{\partial x}, \frac{\partial}{\partial y}, \frac{\partial}{\partial z}\right]}_{\text{Wavelet Transform}}$$

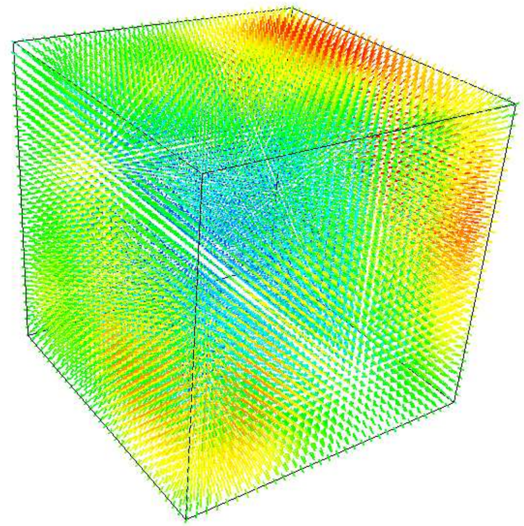

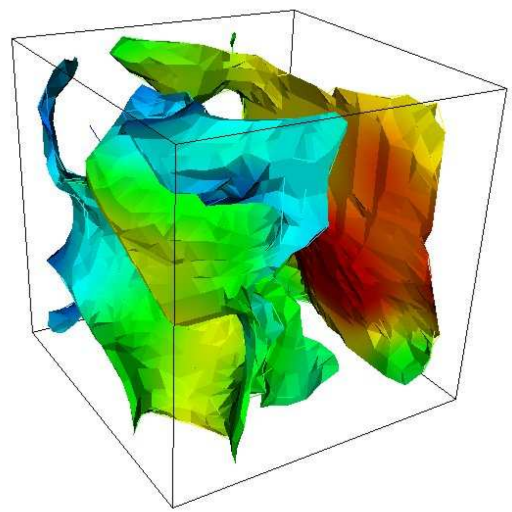

$$\mathbf{T}_\psi(\mathbf{r}, a) = \begin{pmatrix} I * \dfrac{\partial \phi_a}{\partial x}(\mathbf{r}) \\ I * \dfrac{\partial \phi_a}{\partial y}(\mathbf{r}) \\ I * \dfrac{\partial \phi_a}{\partial z}(\mathbf{r}) \end{pmatrix} = \nabla\big(I * \phi_a\big)(\mathbf{r})$$

3D scalar WTMM method : skeleton

WTMM surfaces

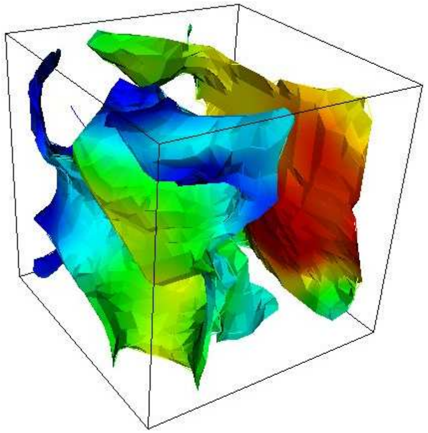

WTMMM points

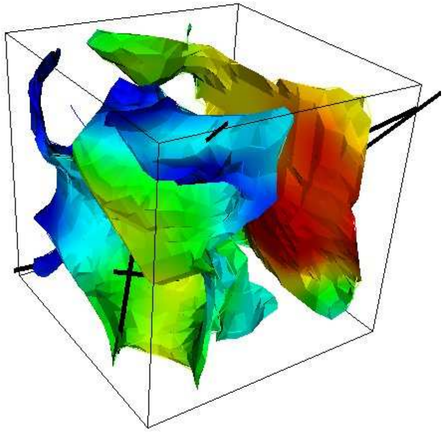

WTMM surfaces at 3 different scales

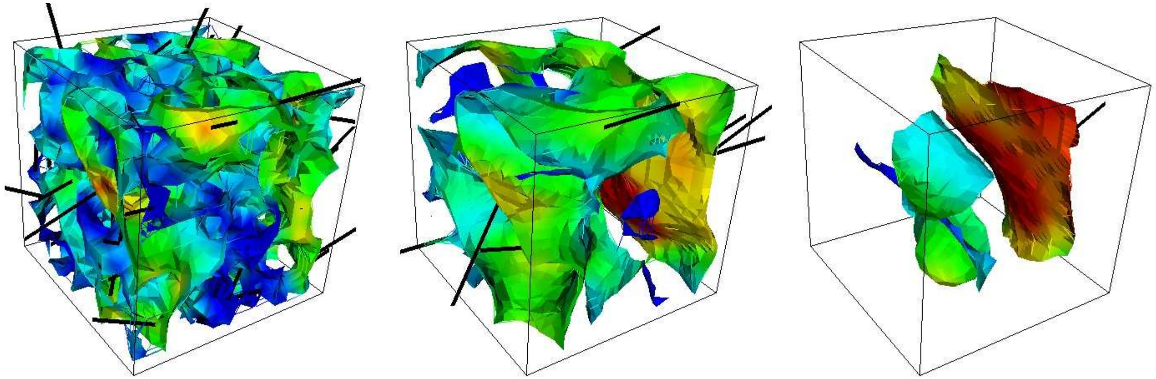

Linking WTMMM : WT Skeleton (projection along z)

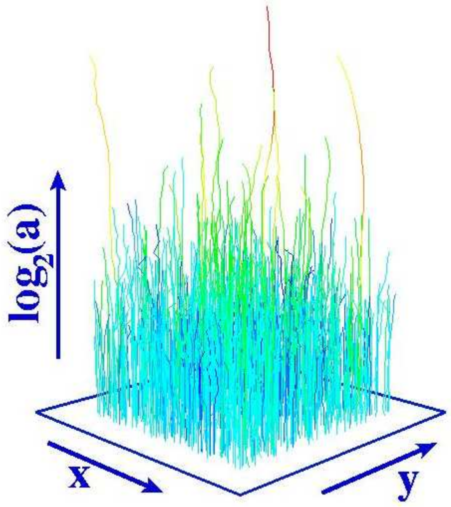

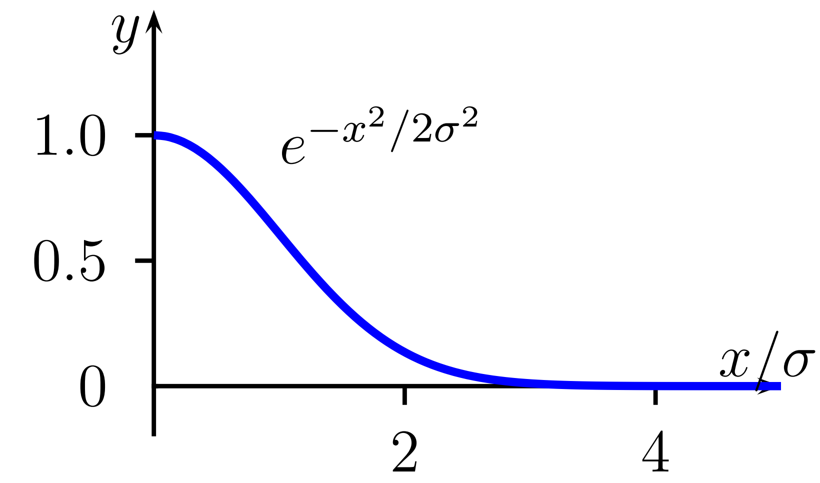

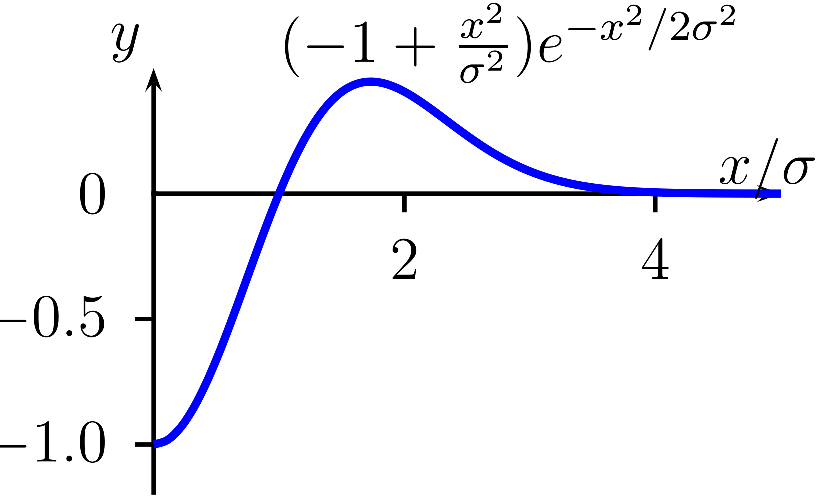

- filters with separated variables
- **Approximate Gaussian filter** $e^{-x^2/2\sigma^2}$ **with** $h_\sigma(x)$
  $$(a_0\cos(\omega_0\tfrac{x}{\sigma}) + a_1\sin(\omega_0\tfrac{x}{\sigma}))\exp^{-b_0\frac{x}{\sigma}} + (c_0\cos(\omega_1\tfrac{x}{\sigma}) + c_1\sin(\omega_1\tfrac{x}{\sigma}))\exp^{-b_1\frac{x}{\sigma}}$$
- **4th order difference equation :**
  $$y_k = n_{00}x_k + n_{11}x_{k-1} + n_{22}x_{k-2} + n_{33}x_{k-3} - d_{11}y_{k-1} - d_{22}y_{k-2} - d_{33}y_{k-3} - d_{44}y_{k-4}$$
- **comparison FFT/recursive filters :**

  computing time decrease in 3D case:

  ☞ **60 % for Gaussian filter**

  ☞ **25 % for Mexican filter**

Test-application to synthetic 3D monofractal fields

fractional Brownian fields : $B_H(\mathrm{r})$

- $H < 0.5$: anti-correlated increments
- $H = 0.5$: non-correlated increments
- $H > 0.5$: correlated increments

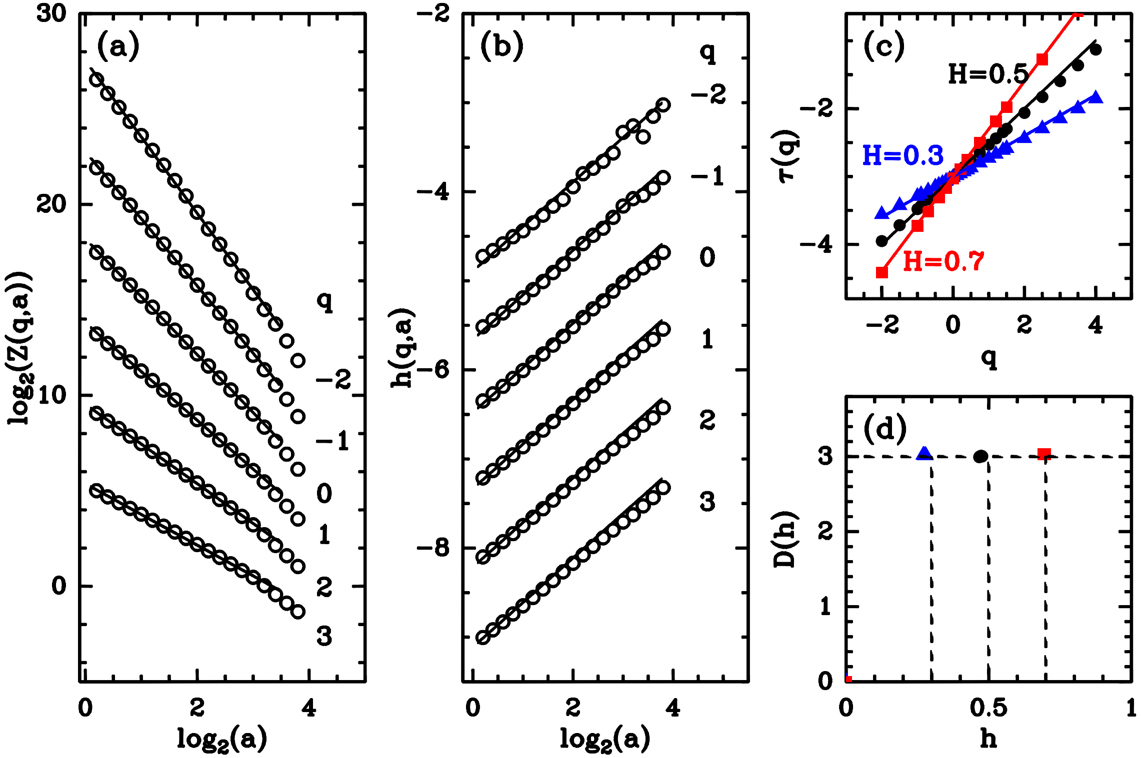

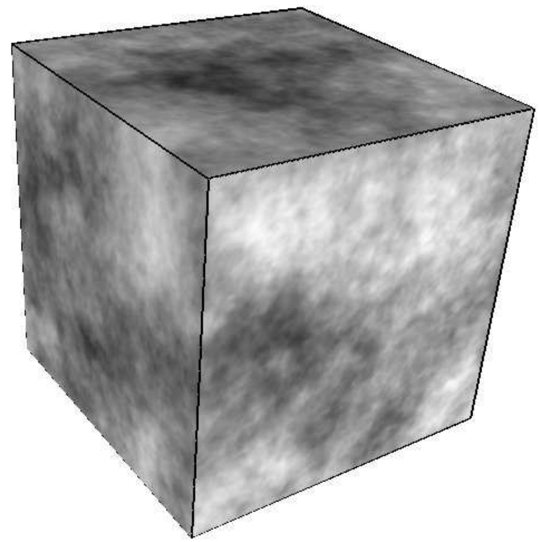

Theoretical predictions :

- $\tau(q)$ is linear:
  $\tau(q) = qH - 3$
- multifractal spectrum is degenerated:
  $D(h = H) = 3$

Test-application to synthetic 3D multifractal fields

3D multifractal fields (Fractionally Integrated Singular Cascades)

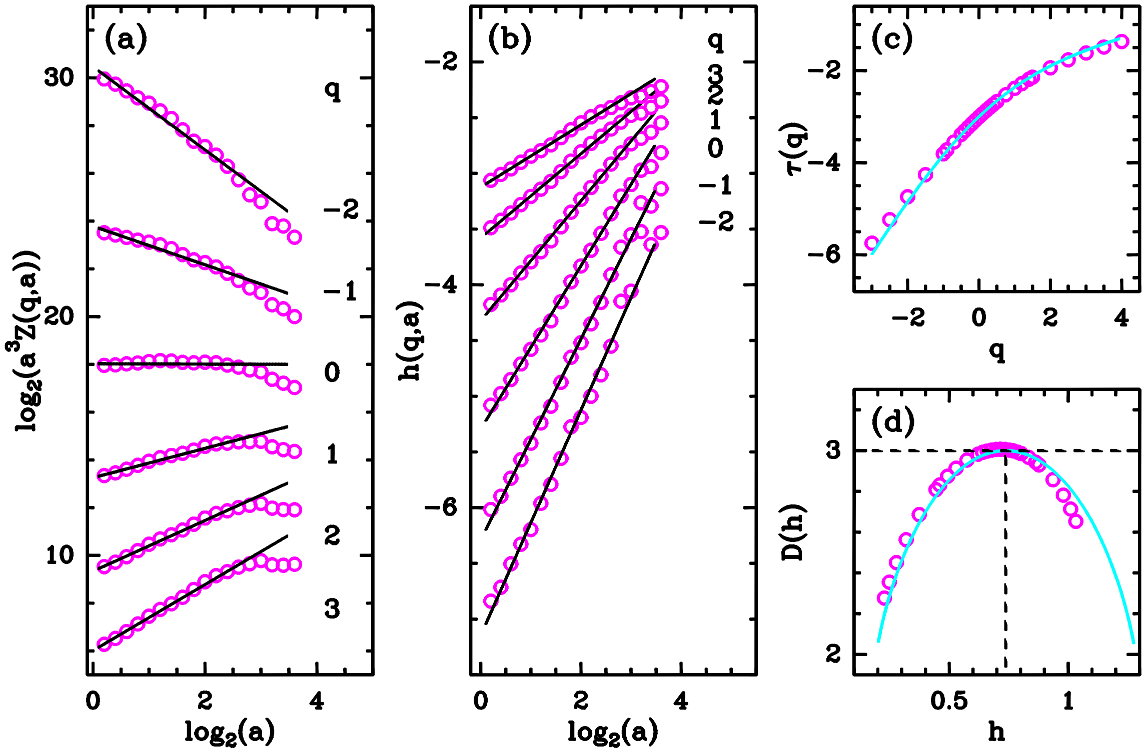

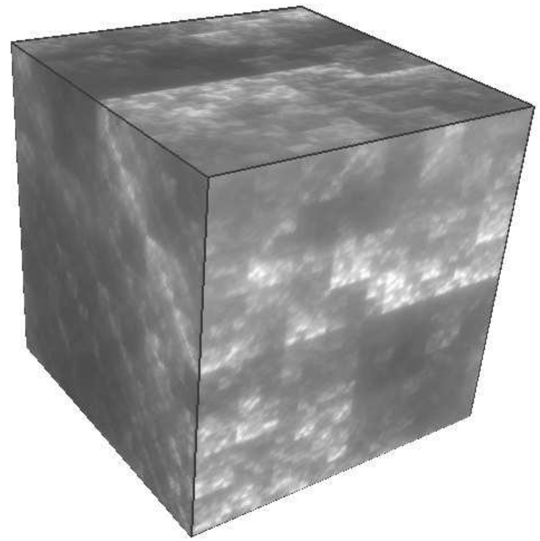

Theoretical predictions :

☞ $$\tau(q) = -2 - q(1 - H^*) - \log_2(p_1{}^q + p_2{}^q).$$
with $p_1 + p_2 = 1$

☞ singularity spectrum is a non-degenerated convexe curve

3D dissipation field : isotropic turbulence DNS

pseudo-spectral code, $(512)^3$ **grid,** $R_\lambda = 216$ **(M. Meneguzzi)**

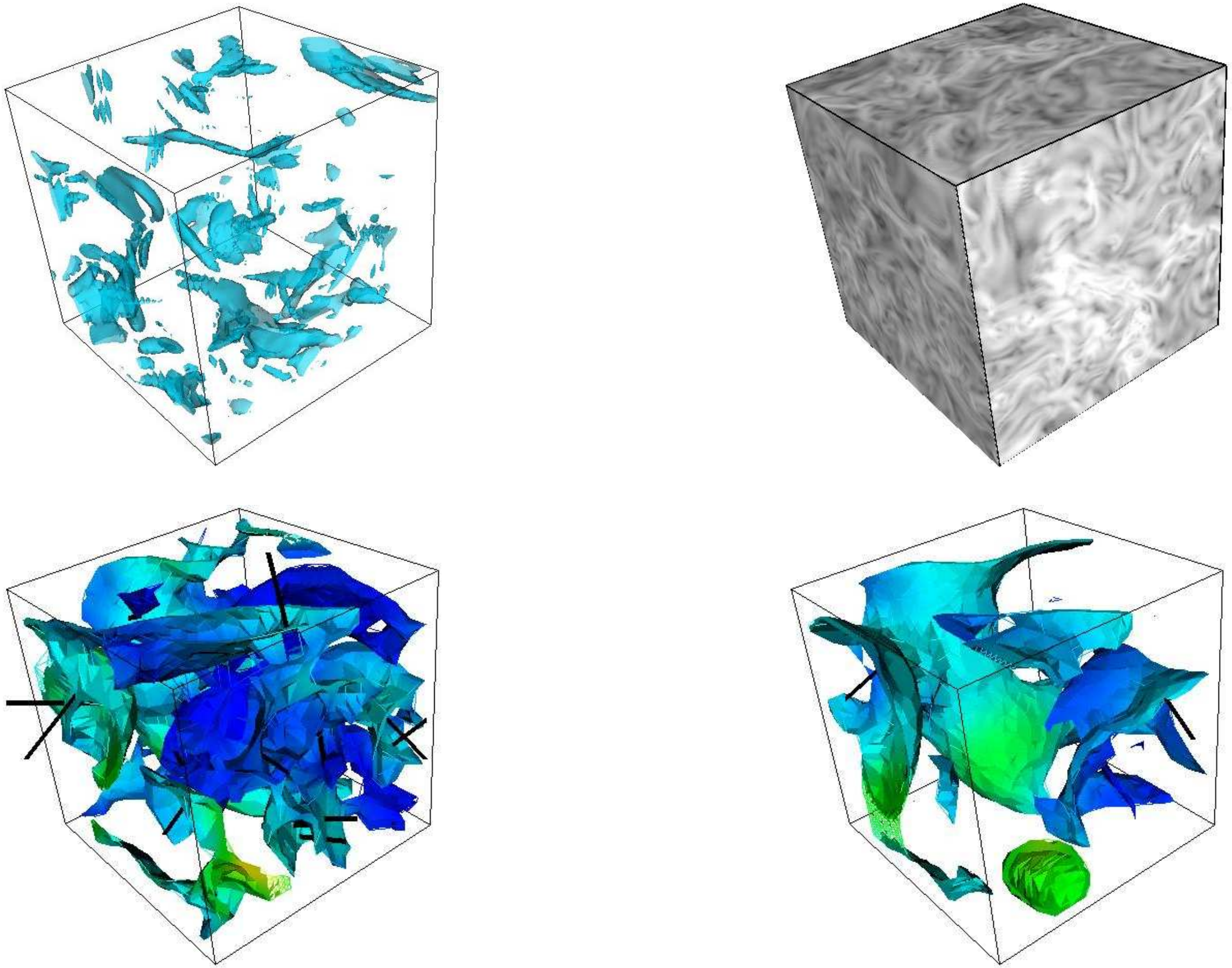

3D WTMM methodology *vs* Box-Counting algorithms

☞ "**Box-Counting**" **algorithm, binomial fit with** $p_1 = 0.3$ **and** $p_2 = 0.7 \rightarrow$ $\boxed{p_1 + p_2 = 1}$ **: diagnoses a conservative multiplicative structure**

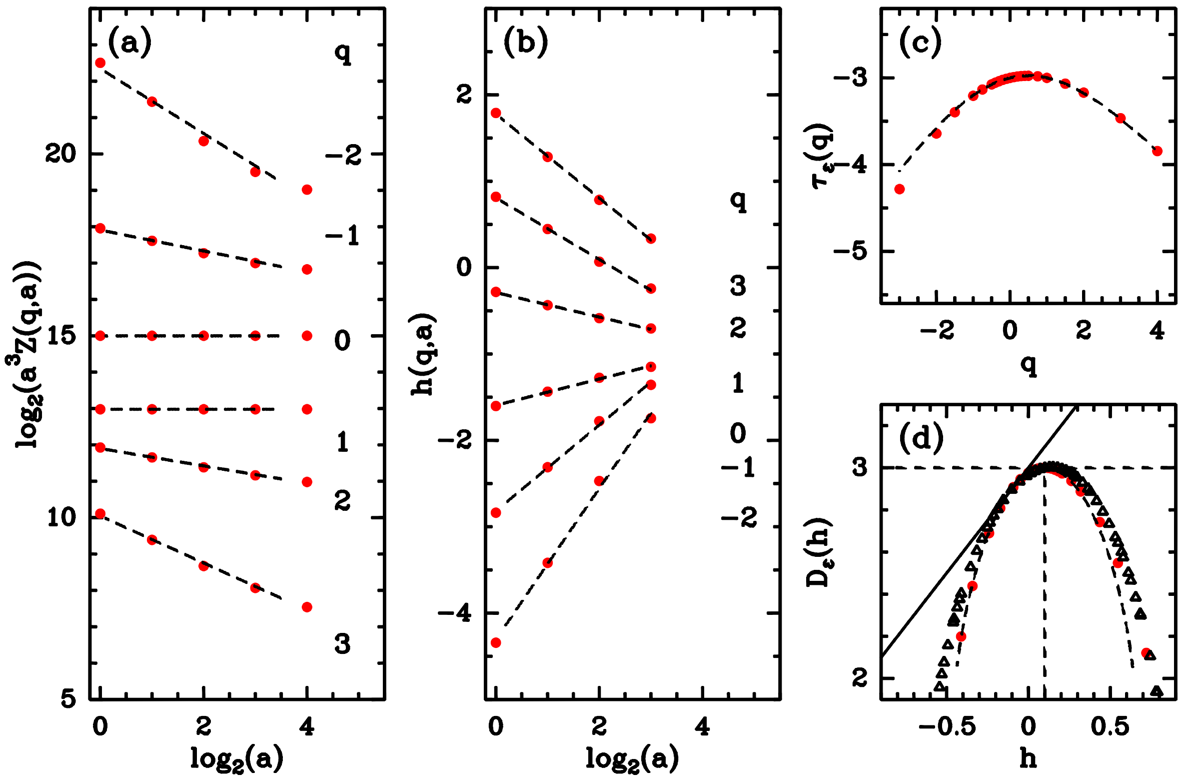

dissipation

binomial model :

$$\tau(q) = -2 - q - \log_2(p_1{}^q + p_2{}^q)$$

3D WTMM methodology *vs* Box-Counting algorithms

- "**Box-Counting**" algorithm, binomial fit with $p_1 = 0.3$ and $p_2 = 0.7 \rightarrow$ $\boxed{p_1 + p_2 = 1}$: diagnoses a **conservative** multiplicative structure
- "**3D WTMM**" method reveals a **non-conservative** multiplicative structure : binomial fit with $p_1 = 0.36$ and $p_2 = 0.80 \Rightarrow \boxed{p_1 + p_2 \neq 1}$

dissipation

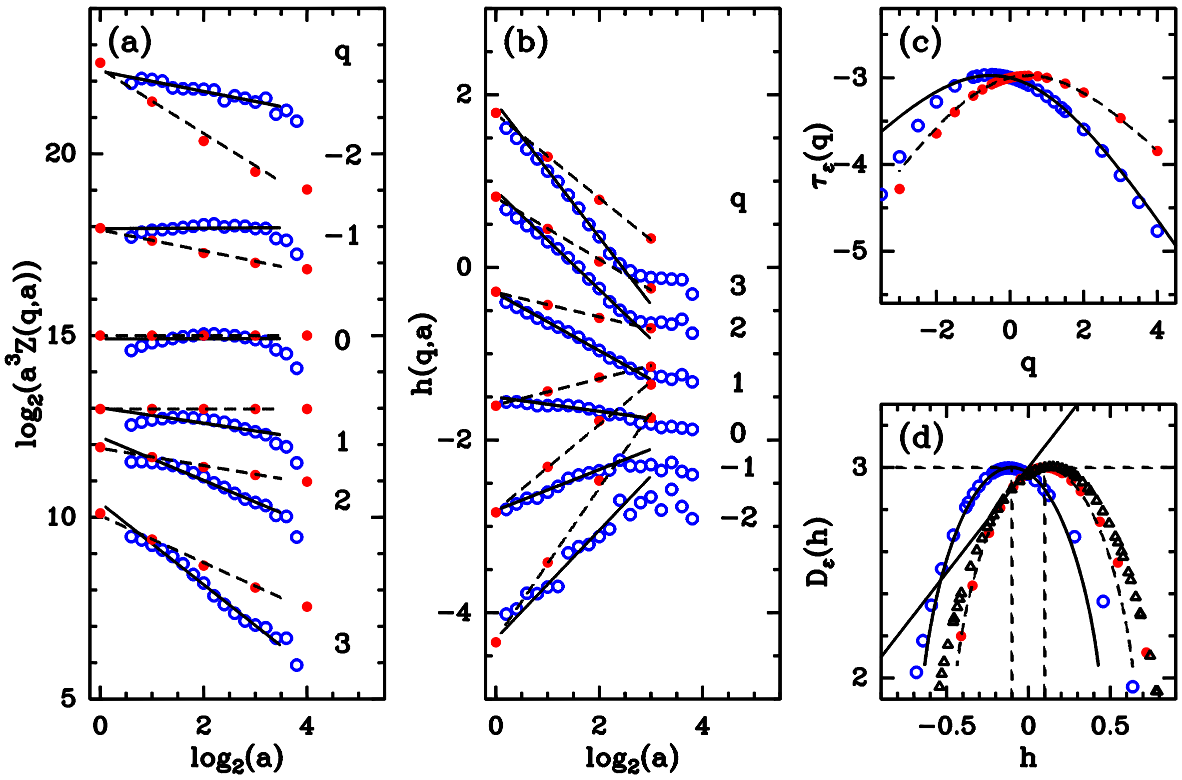

binomial model :

$$\tau(q) = -2 - q - \log_2(p_1{}^q + p_2{}^q)$$

remark:

$$p_1 = \frac{p_1}{p_1 + p_2}$$

$\Rightarrow$ inconsistent box-counting !

Comparative 3D WTMM analysis of dissipation and enstrophy

☞ **Dissipation**, **non-conservative** multiplicative structure :

binomial fit with $p_1 = 0.36$ and $p_2 = 0.80 \Rightarrow \boxed{p_1 + p_2 = 1.16}$

☞ **Enstrophy**, **non-conservative** multiplicative structure :

binomial fit with $p_1 = 0.38$ and $p_2 = 0.94 \Rightarrow \boxed{p_1 + p_2 = 1.32}$

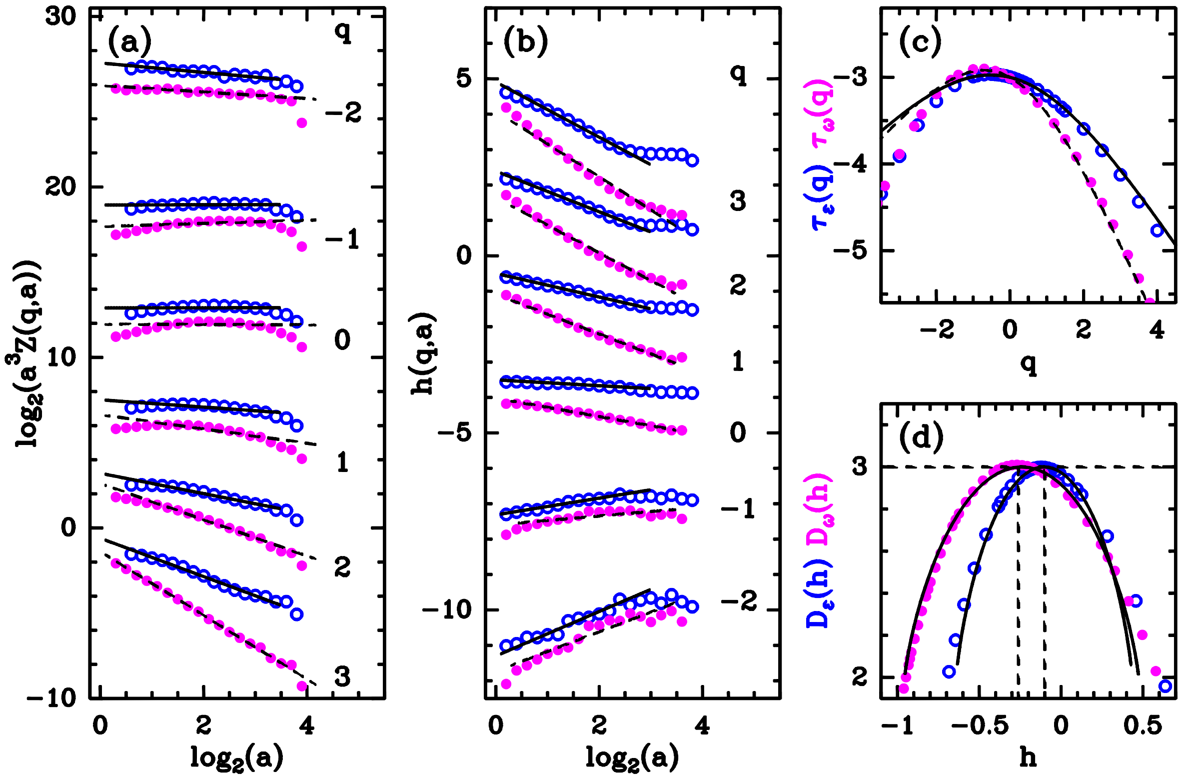

Intermittency coefficients:

- Dissipation : $C_2 \sim 0.22$
- Enstrophy : $C_2 \sim 0.30$

Self-similar multifractal vector-valued measure (2D case)

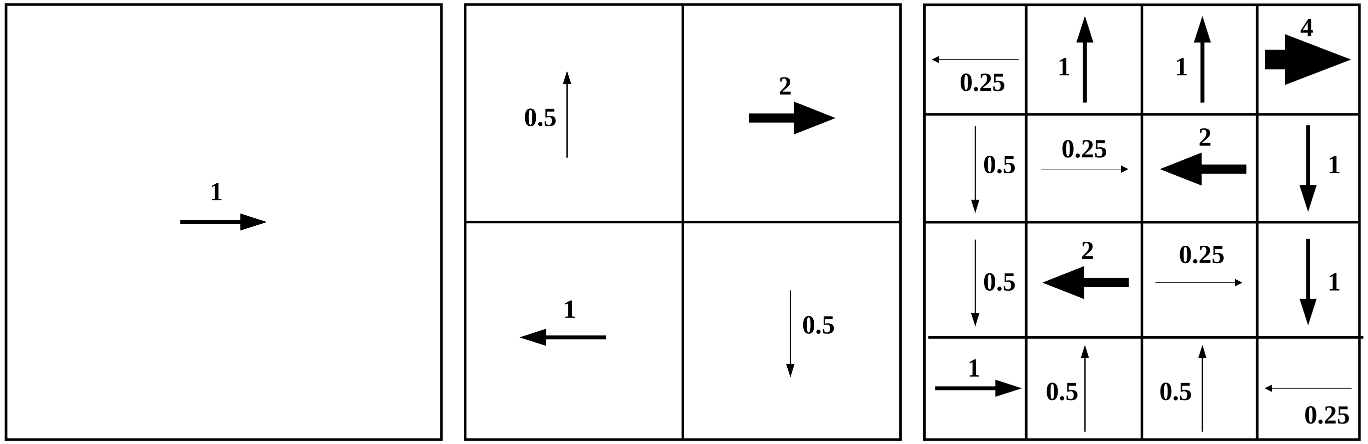

- ☞ **Falconer and O'Neil (1995)**
- ☞ **scalar measure** $\{\mathrm{r} : \lim_{l \to 0} \frac{\log \mu(B(\mathrm{r}, l))}{\log l} = \alpha\}, \quad \alpha = h + 2$

$$\mathcal{Z}(q, l) = \sum_i \mu_i^q(l) \sim l^{\tau_\mu(q)}$$

- ☞ **vector-valued measure** $\left\{\mathrm{r} : \lim_{l \to 0} \frac{\log \int_{B(\mathrm{r}, l)} ||\Phi_l \mu(\mathrm{s})|| d\mathcal{L}_d(\mathrm{s})}{\log l} = \alpha\right\}, \quad \alpha = h + 2$

$$\mathcal{Z}(q, l) = \sum_i ||\Phi_l \mu||_i^q \sim l^{\tau_\mu(q)}$$

Self-similar multifractal <u>vector-valued</u> measure (2D case)

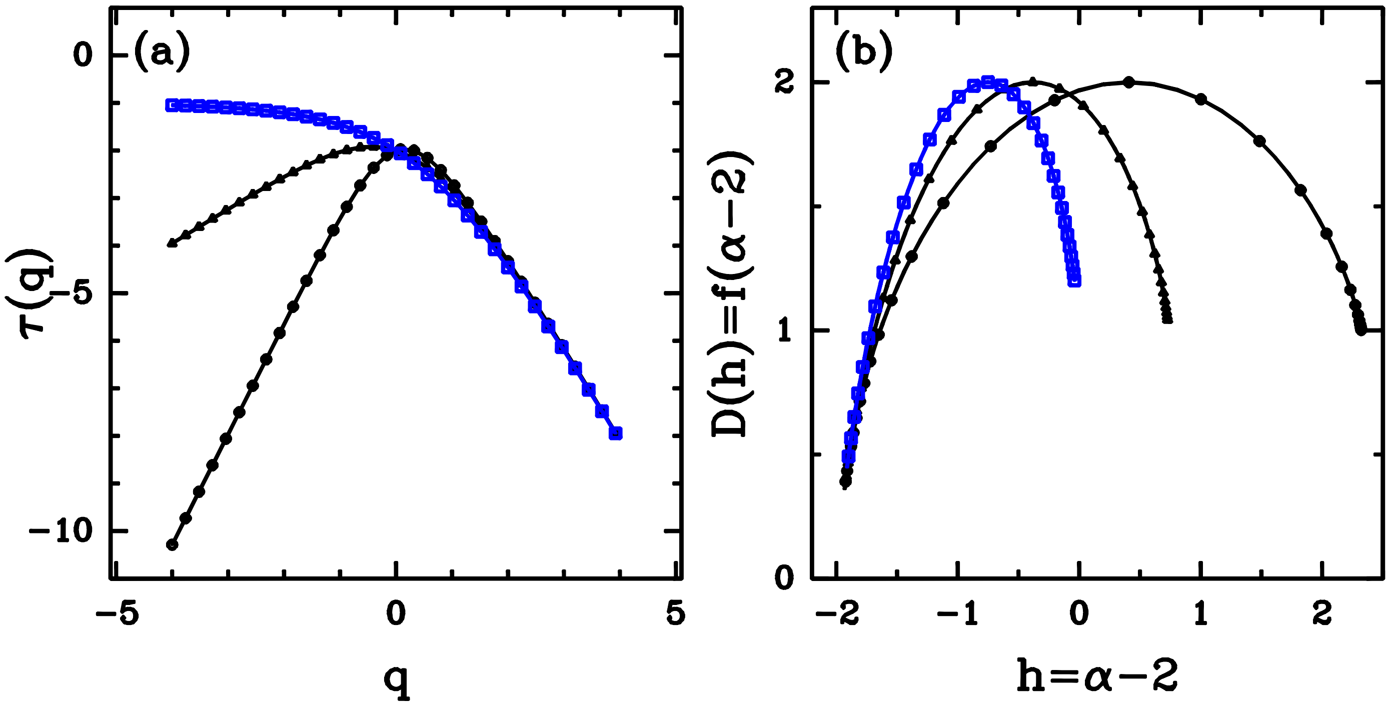

☞ $\tau_{\mu}(q) = -\frac{\log(p_1^q + p_2^q + p_3^q + p_4^q)}{\log 2}$

☞ $D_{\mu}(h) = f_{\mu}(\alpha - 2) = \inf_q (qh - \tau_{\mu}(q))$.

Tensorial wavelet transform (2D case)

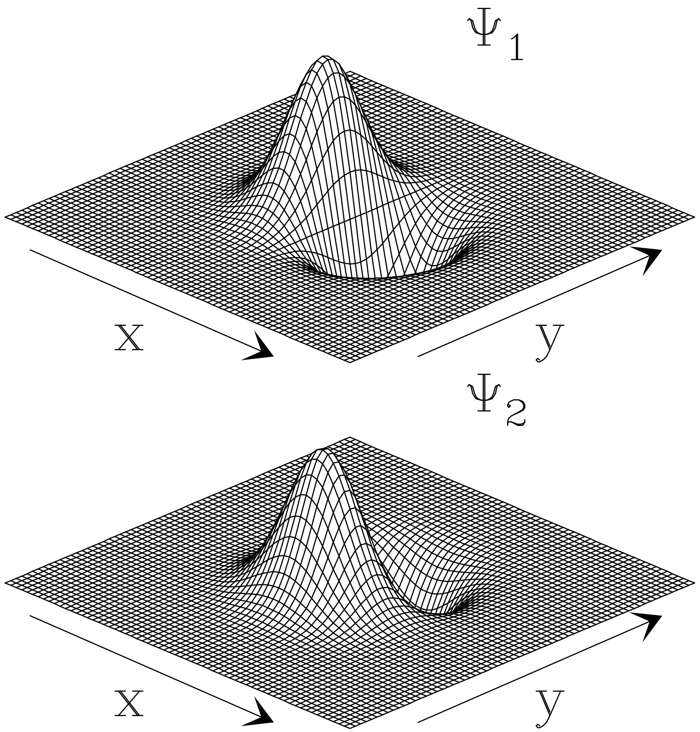

1. **Tensorial wavelet transform of field $\mathbf{V} = (V_1, V_2)$:**

$$\mathbb{T}_{\psi}[\mathbf{V}](\mathbf{b}, a) = (\mathbf{T}_{\psi_i}[V_j](\mathbf{b}, a)) = \begin{pmatrix} T_{\psi_1}[V_1] & T_{\psi_1}[V_2] \\ T_{\psi_2}[V_1] & T_{\psi_2}[V_2] \end{pmatrix}$$

$$T_{\psi_i}[V_j](\mathbf{b}, a) = a^{-2} \int d^2x\mathbf{r}\ \psi_i\left(a^{-1}(\mathbf{r} - \mathbf{b})\right) V_j(\mathbf{r}), j = 1, 2$$

2. **Direction of greatest variation of vector field :**

$$|\mathbb{T}_{\psi}[\mathbf{V}]| = \sup_{\mathbf{C} \neq 0} \frac{||\mathbb{T}_{\psi}[\mathbf{V}].\mathbf{C}||}{||\mathbf{C}||}$$

3. **Singular value decomposition of WT tensor:**

$$\mathbb{T}_{\psi}[\mathbf{V}] = \left(G\right) .\begin{pmatrix} \sigma_{\max} & 0 \\ 0 & \sigma_{\min} \end{pmatrix}. \left(D\right)^T$$

4. **Tensorial wavelet transform** :

$$\mathbf{T}_{\psi,\max}[\mathbf{V}](\mathbf{b}, a) = \sigma_{\max} \mathbf{G}_{\sigma_{\max}}$$

Tensorial 2D WTMM methodology

Data

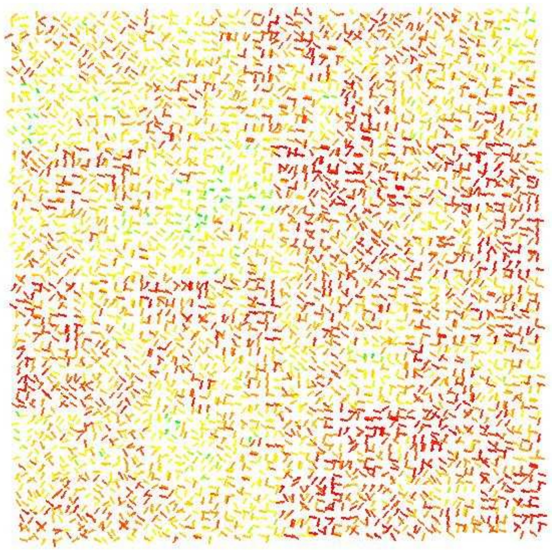

Tensorial wavelet transform

$$\mathbf{T}_{\boldsymbol{\psi},\max}[\mathbf{V}](\mathbf{b}, a) = \sigma_{\max}\mathbf{G}_{\sigma_{\max}}$$

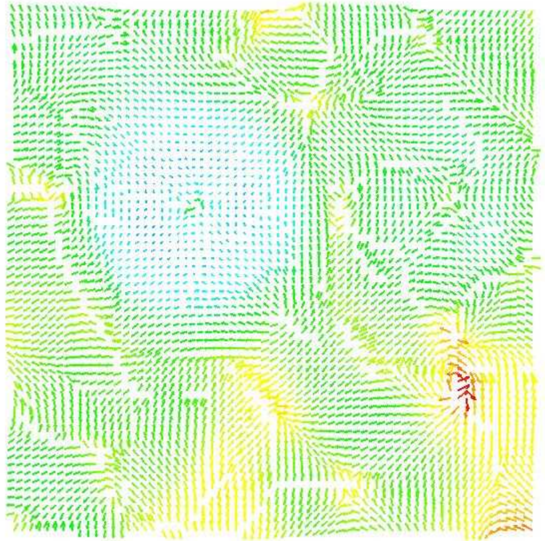

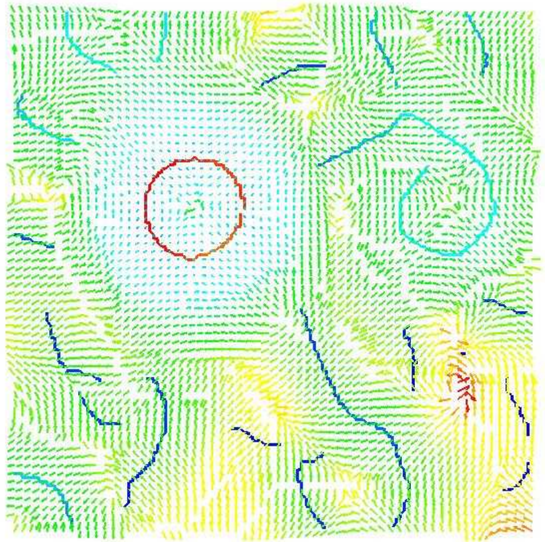

Modulus Maxima $\boldsymbol{\sigma}_{\mathbf{max}}$ chains of tensorial wavelet transform at scale a :

$$\left\{ (\boldsymbol{b}, \boldsymbol{a}) / \frac{\partial \boldsymbol{\sigma}_{\mathbf{max}}}{\partial \boldsymbol{G}_{\mathbf{max}}} = 0 \quad \text{et} \quad \frac{\partial^2 \boldsymbol{\sigma}_{\mathbf{max}}}{\partial \boldsymbol{G}^2_{\mathbf{max}}} < 0 \right\}$$

Tensorial 2D WTMM methodology: Skeleton

WTMM Chains

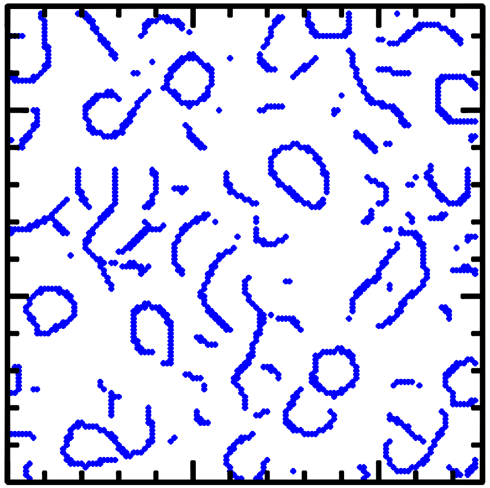

WTMMM

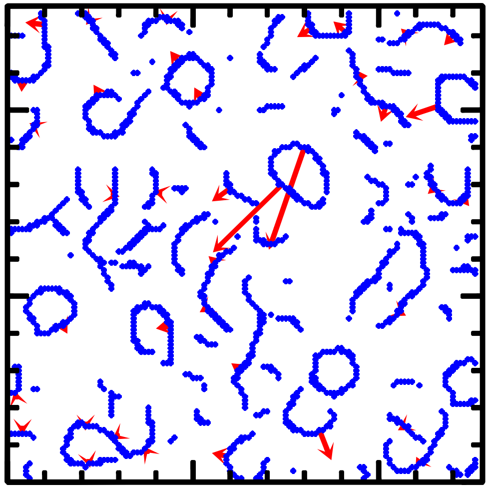

WTMM Chains at 3 different scales

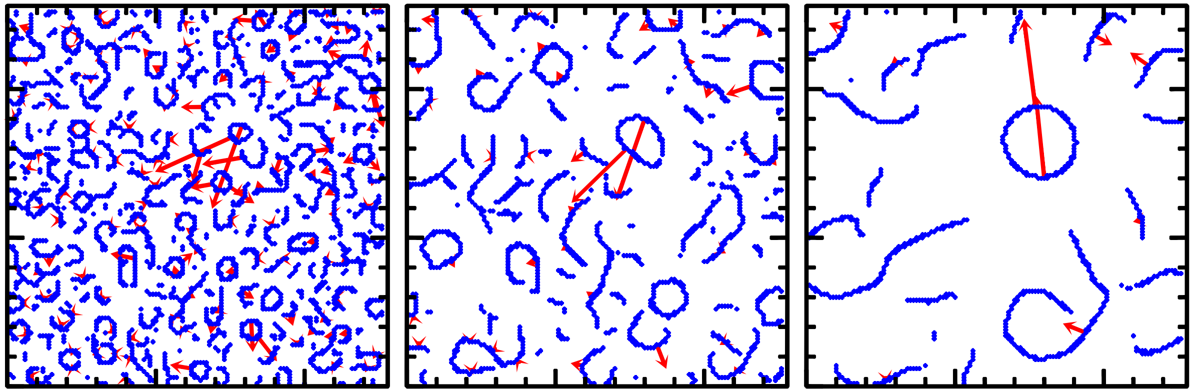

WTMMM linking: WT Skeleton

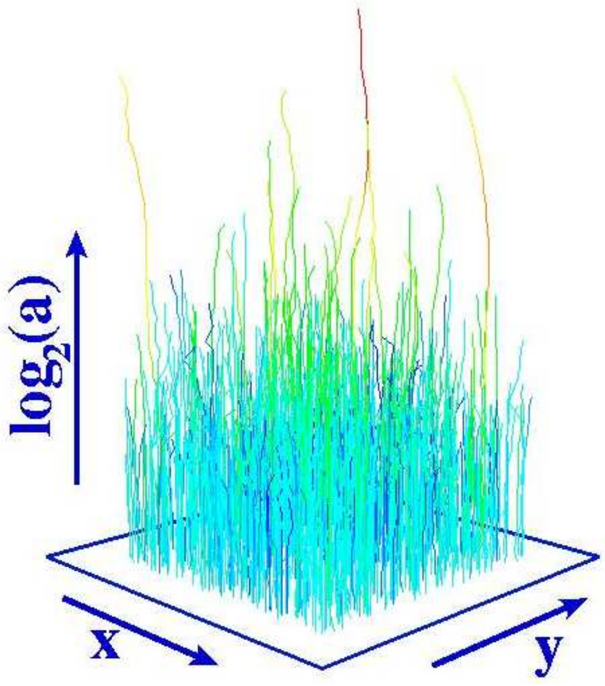

Monofractal 2D vector fields

fractional Brownian fields : $\mathrm{B}_{H}(\mathrm{r})$

☞ **Spectral method simulation**

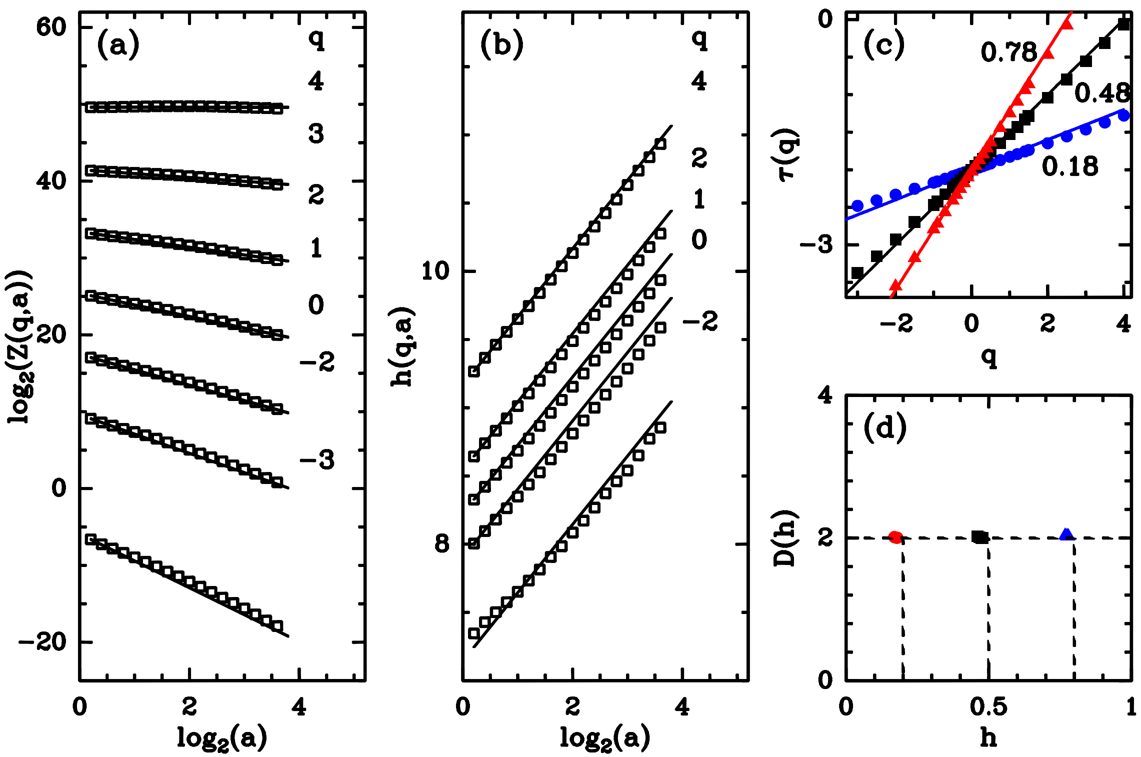

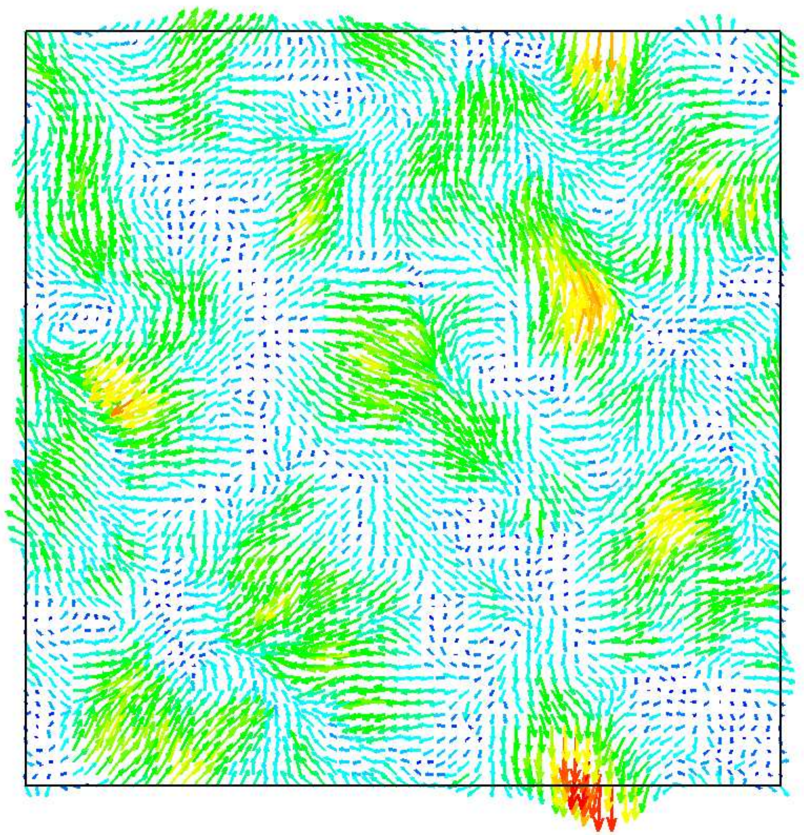

Theoretical predictions :

- **linear** $\tau(q)$: $\tau(q) = qH - 2$
- **degenerated singularity spectrum:**
  $D(h = H) = 2$

2D self-similar multifractal vector-valued measures

Self-similar multifractal vector-valued measures (Falconer and O'Neil's model)

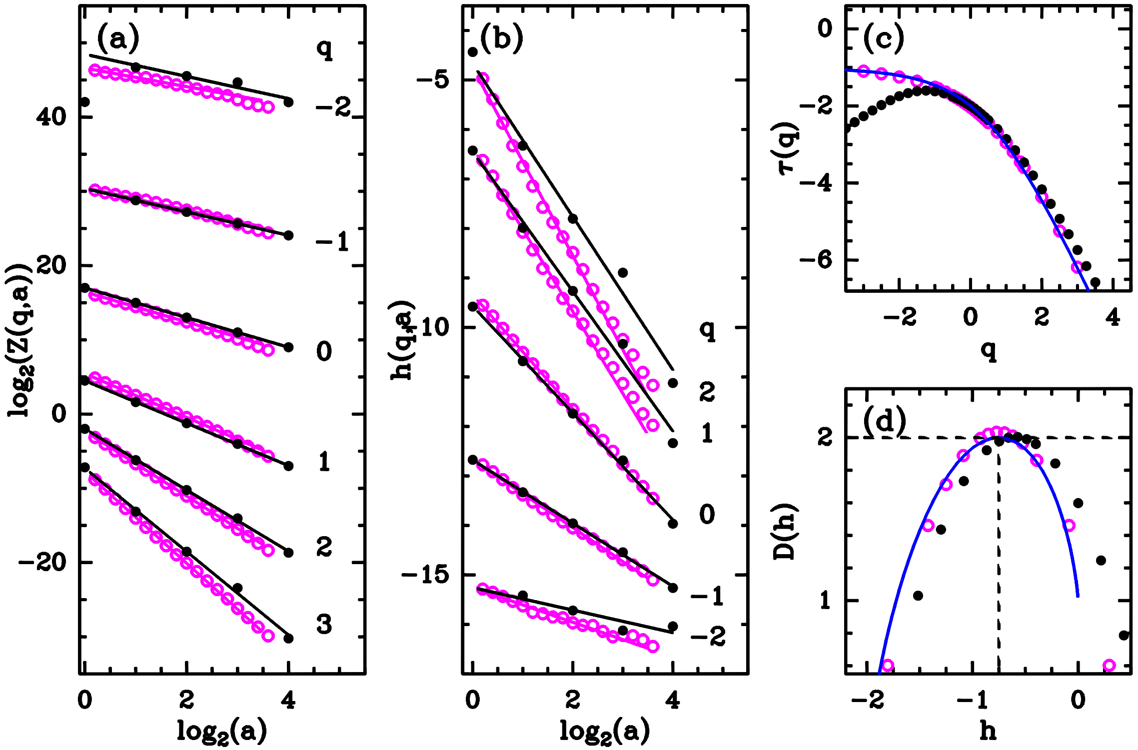

● vectorial box-counting

○ vectorial 2D WTMM method

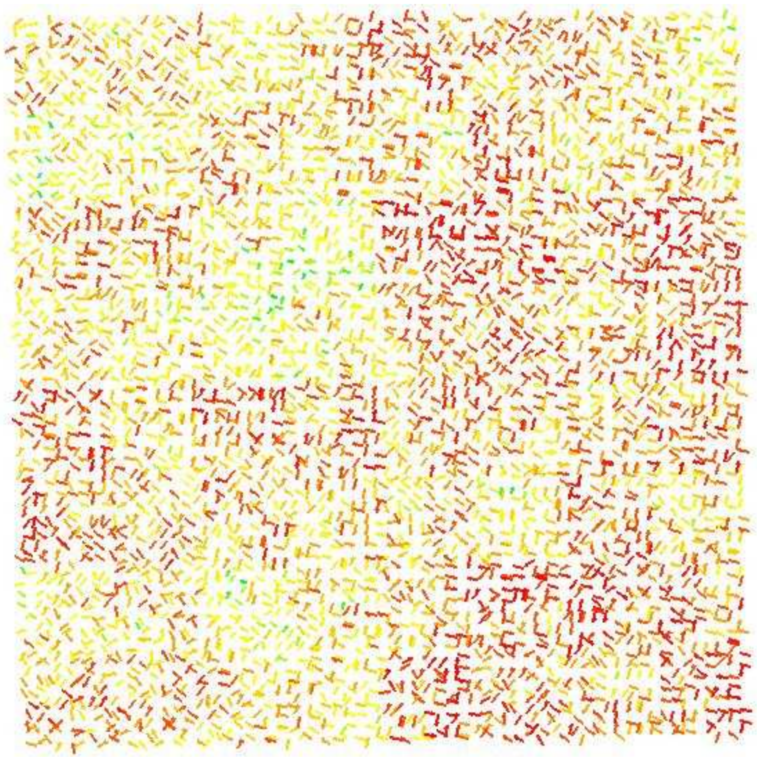

Theoretical predictions:

- $\tau(q) = -\log_2(p_1{}^q + p_2{}^q + p_3{}^q + p_4{}^q)$
  $p_1 = p_4 = 0.5$, $p_2 = 2$ and $p_3 = 1$
- **vectorial box-counting is less accurate**

Tensorial 3D WTMM method: turbulent velocity field ($R_\lambda = 140$)

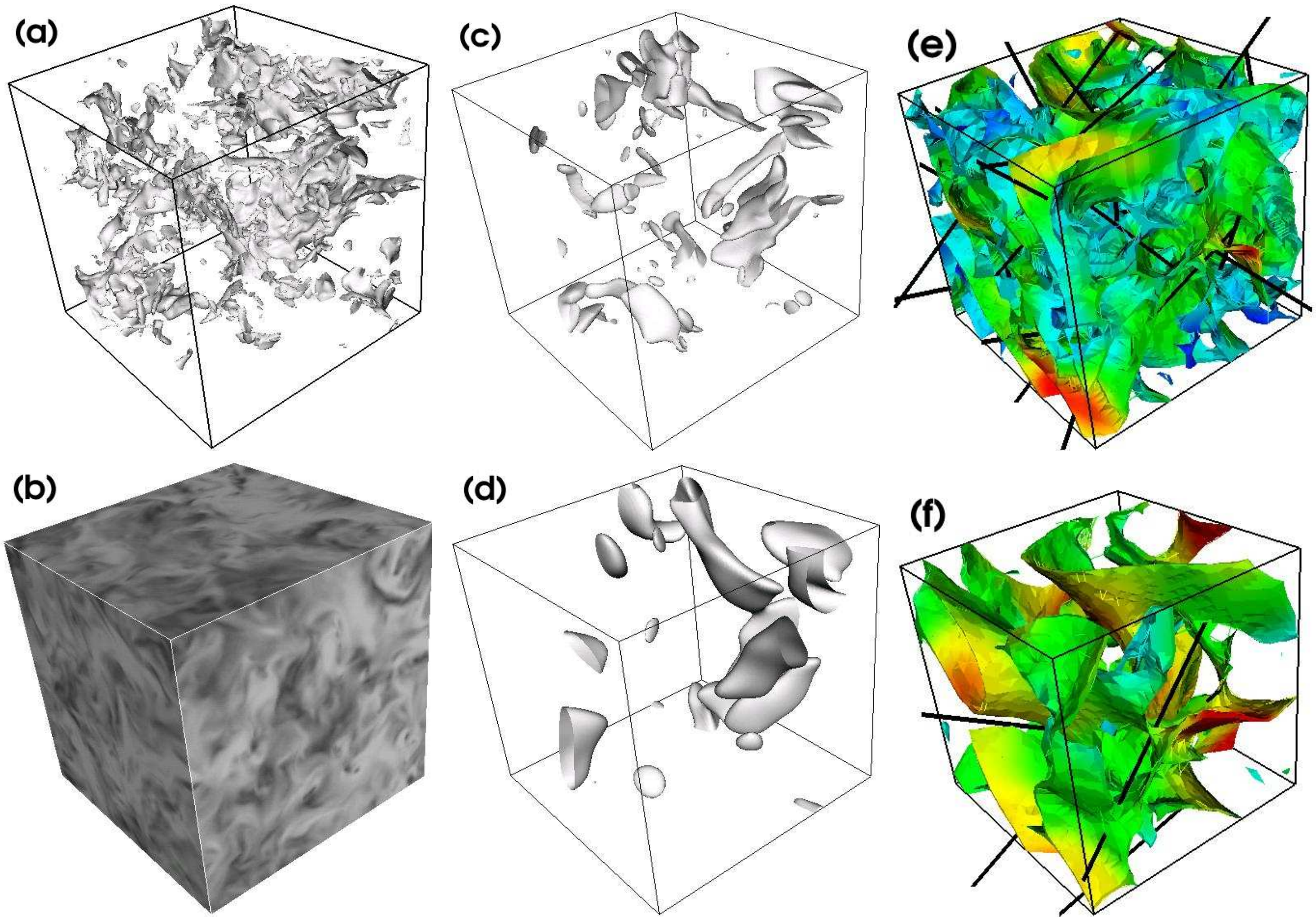

Tensorial 3D WTMM method: singularity spectrum of velocity

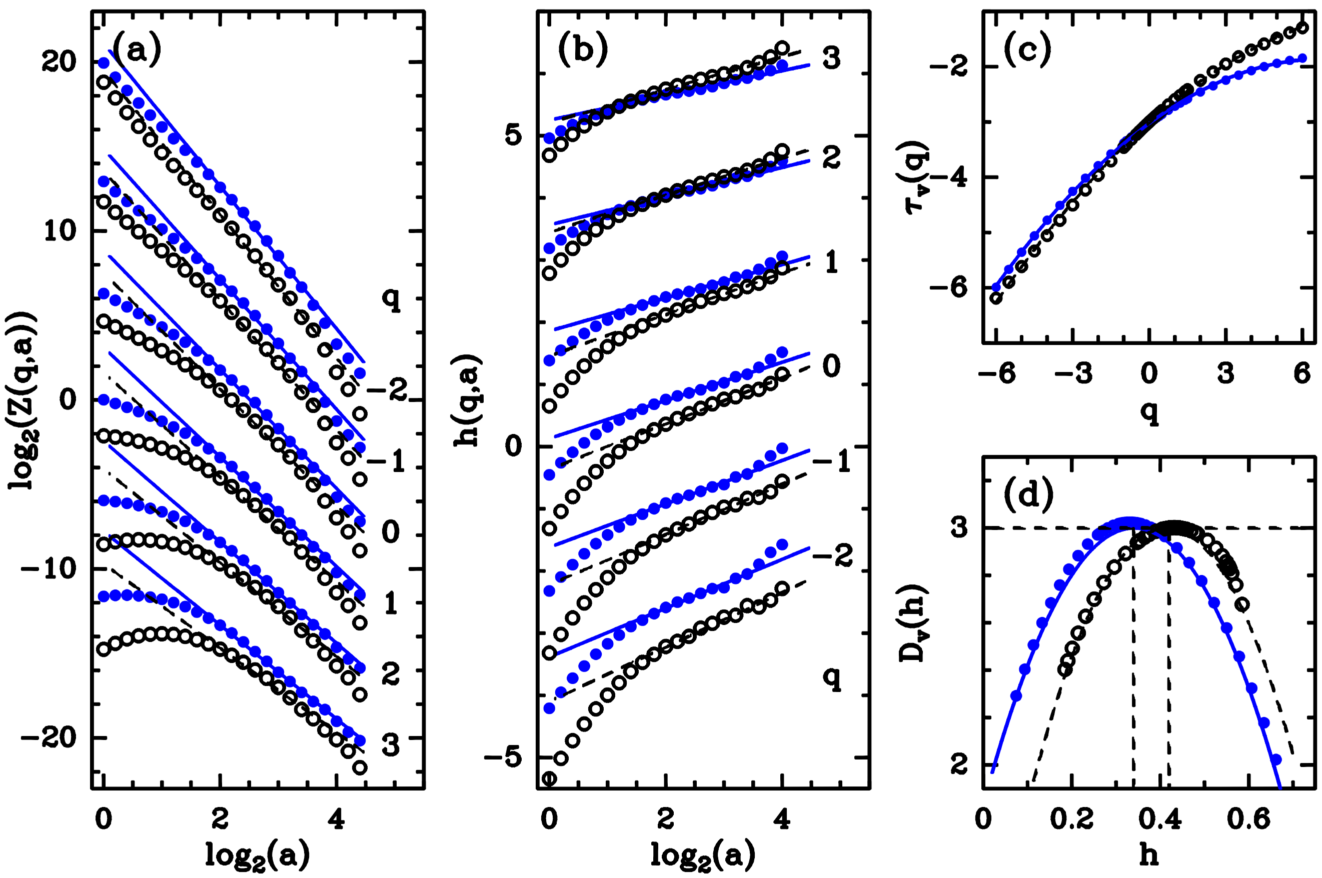

- parabolic fi t : $\tau(q) = -C_0 - C_1 q - C_2 \frac{q^2}{2}$
- intermittency coeffi cient $C_2 = 0.049 \pm 0.004$

1D increments method:

- longitudinal : $C_2(\delta v_L) \sim 0.025$

  transverse : $C_2(\delta v_T) \sim 0.040$

Tensorial 3D WTMM method: turbulent velocity field ($R_\lambda = 140$)

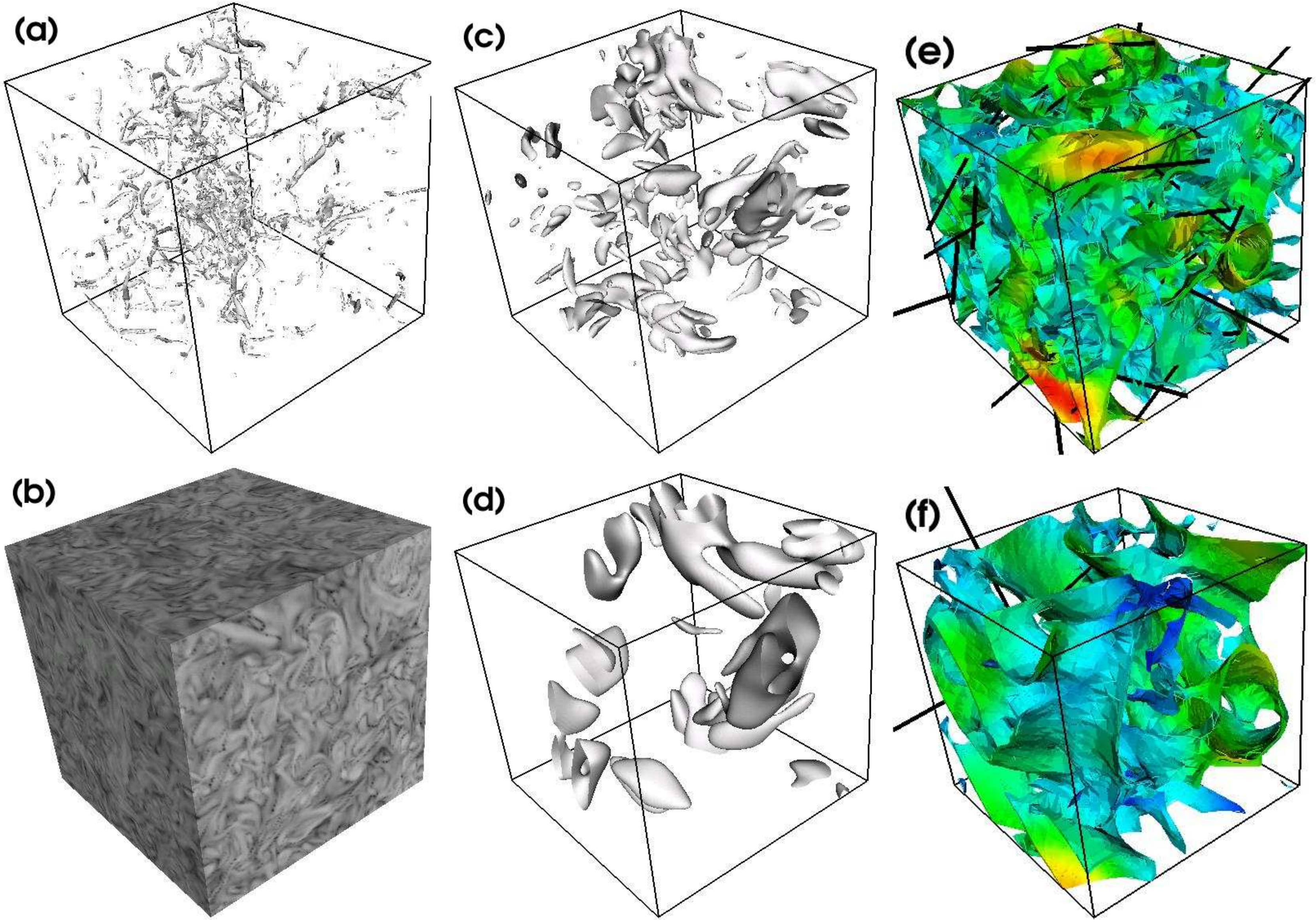

Tensorial 3D WTMM method: singularity spectrum of vorticity

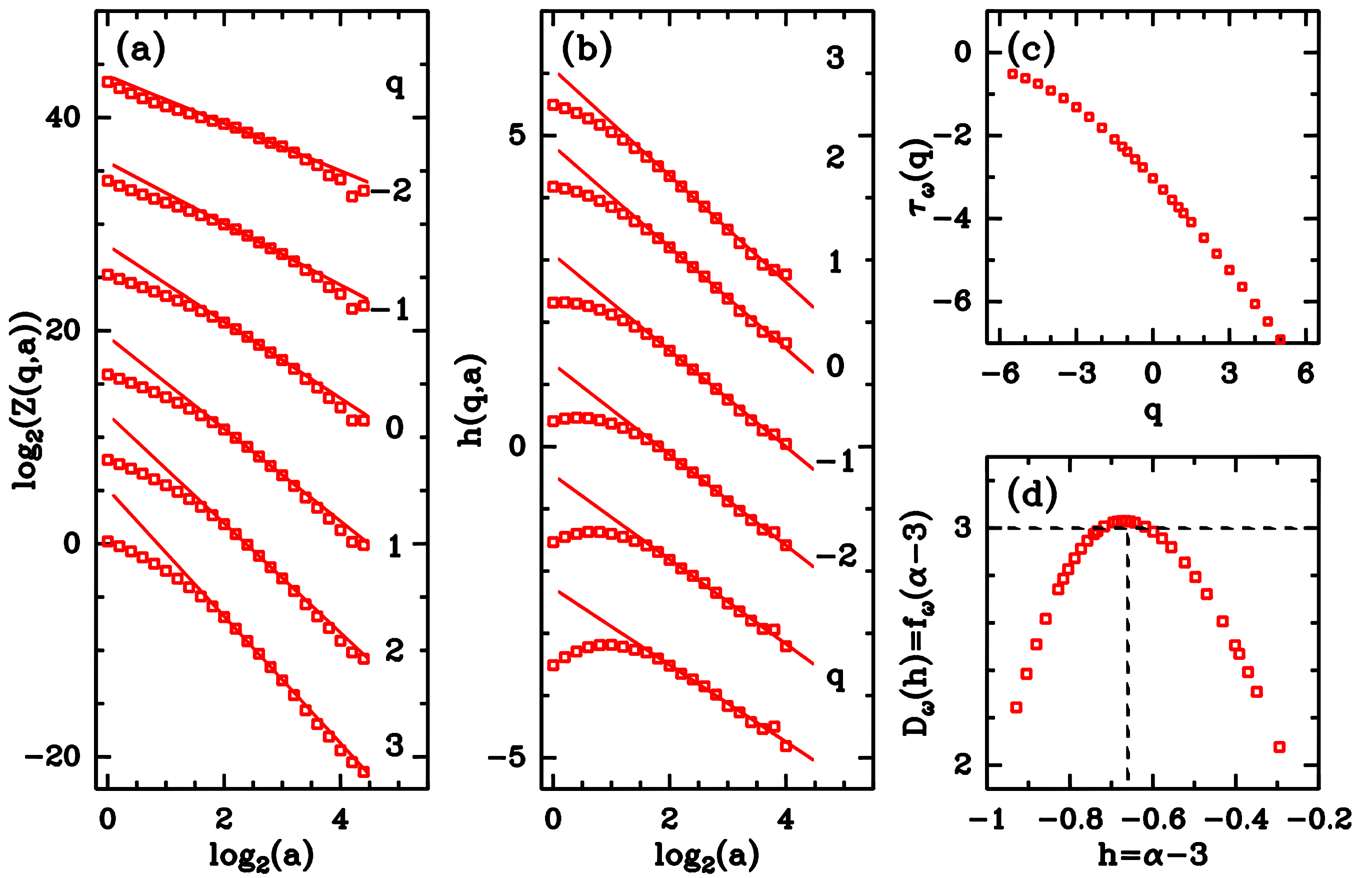

- □ vorticity

Tensorial 3D WTMM method: singularity spectrum of vorticity

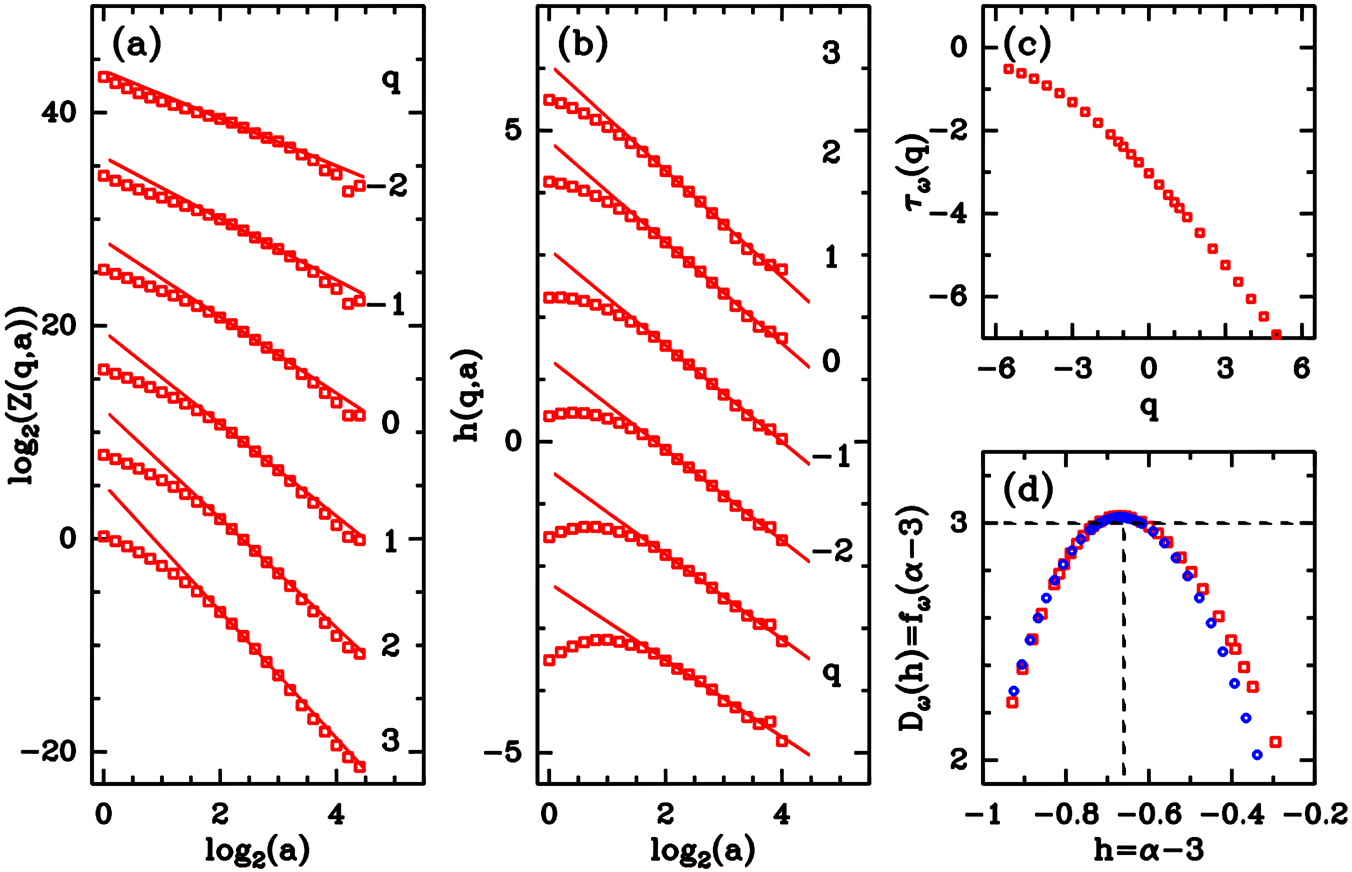

□ vorticity

○ $D_v(h+1)$ spectrum translated velocity

$\Rightarrow$ same 3D intermittency coefficient !

Conclusion

assessment:

- **WTMM multifractal analysis: moving towards vector fields**

outlooks :

- **better understanding of the information embedded in the WT tensor.**
- **identification of coherent structures in turbulence using WT tensor's smallest singular value: vorticity filaments or sheets.**
- **others applications : astrophysics (interstellar medium, interstellar turbulence), MHD, geophysics, ...**

Thanks :

- **E. Lévêque, Laboratoire de Physique, ENS Lyon (Turbulent flows DNS).**

References :

- **P. Kestener and A. Arneodo,** *Phys. Rev. Lett.*, **91:194501, 2003.**
- **P. Kestener and A. Arneodo,** *Phys. Rev. Lett.*, **93:044501, 2004.**

Preliminary results :

Isosurface plots of data and 3D WT modulus (Gaussian filtering) :

$z = 5$ $z = 2$ $z = 0$

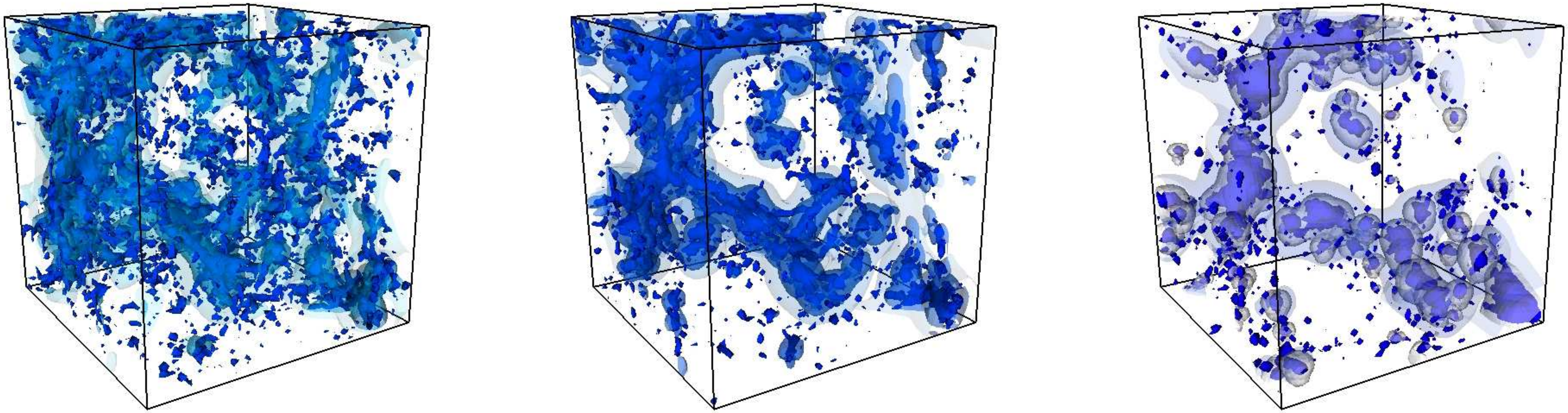

3D Box-Counting method: singularity spectrum ($z = 0$ and $z = 5$)

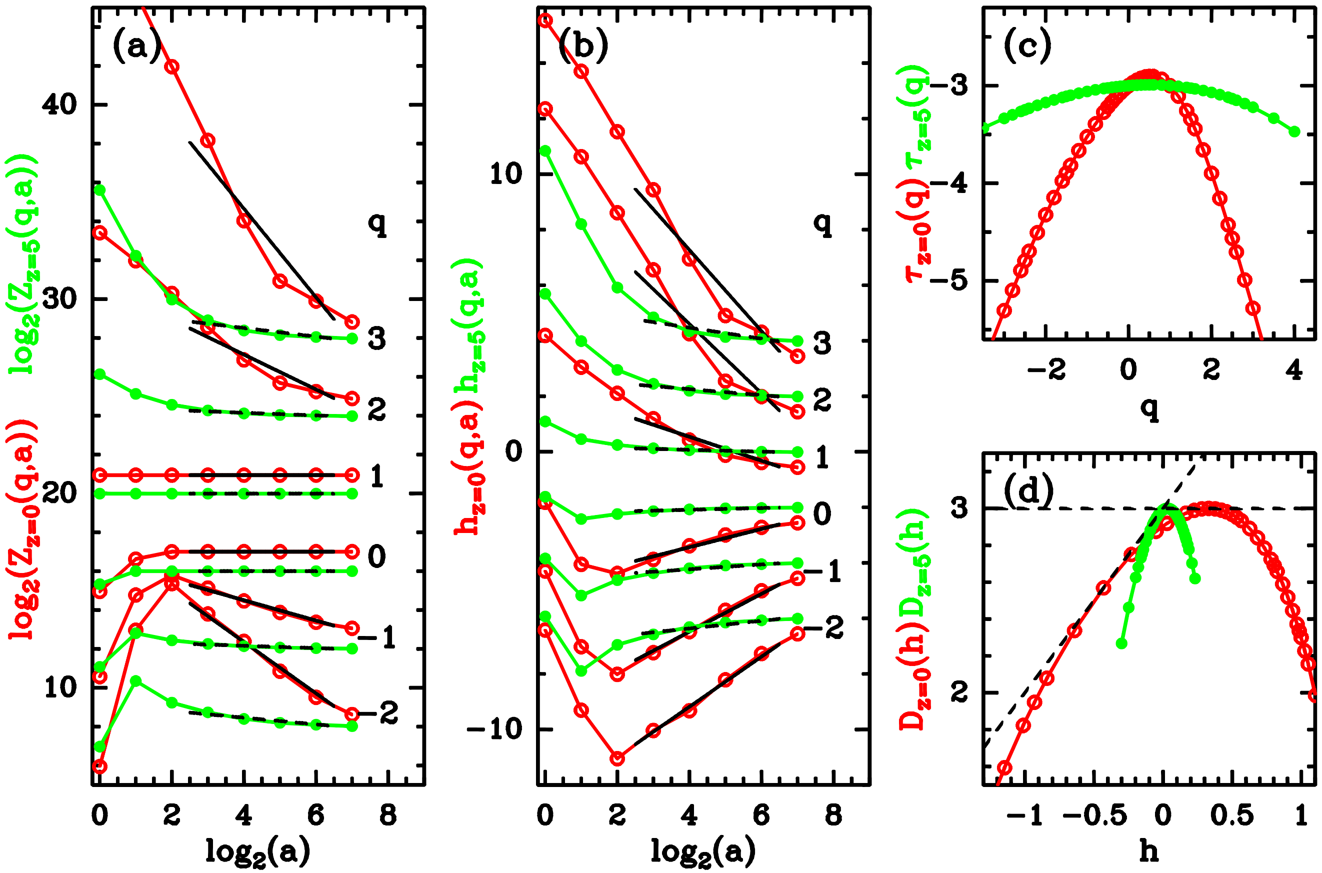

- NO CLEAR SCALING !!!
- perhaps scaling at large scales ??

Scalar 3D WTMM method: singularity spectrum ($z=0$ and $z=5$)

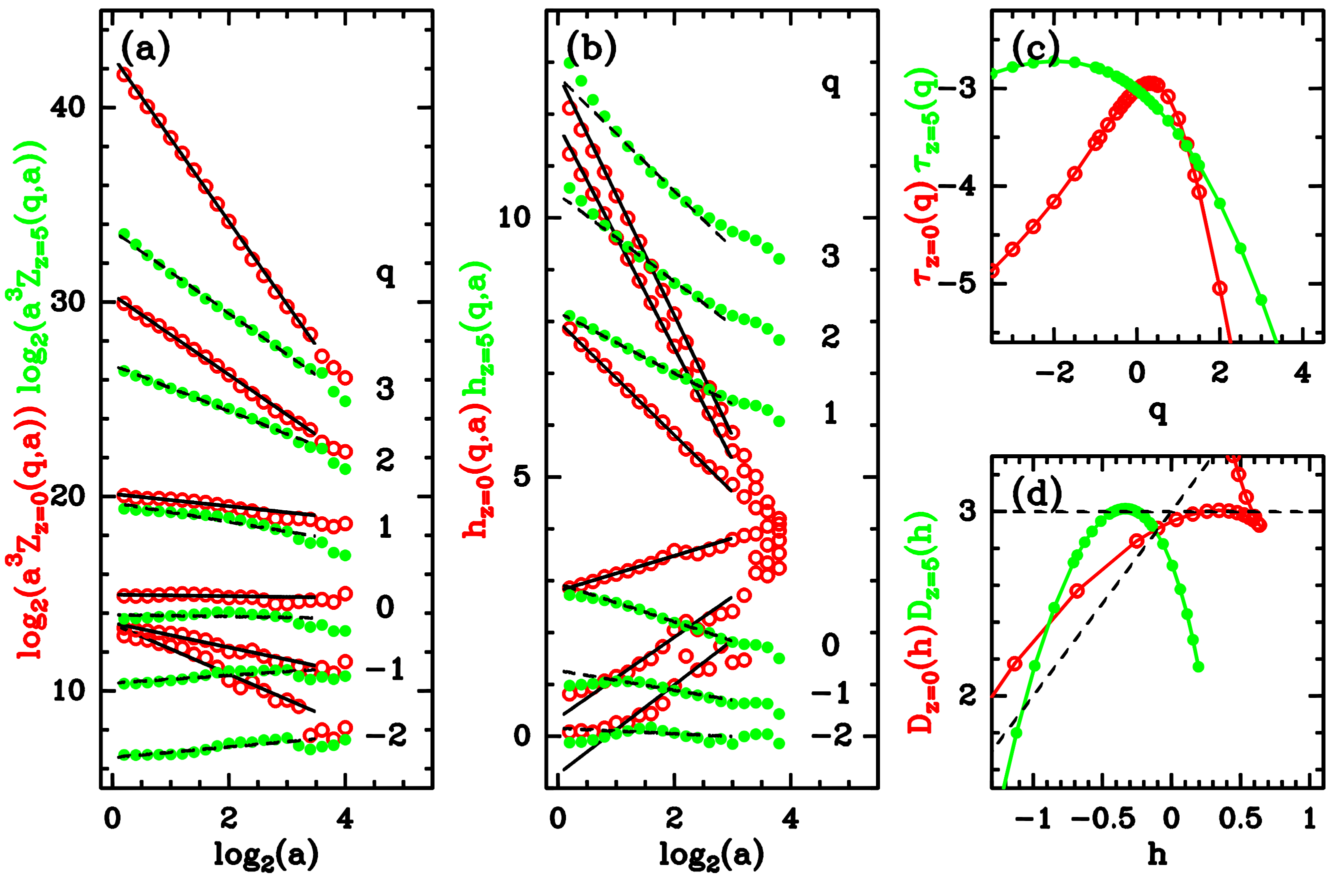

- parabolic fi t : $\tau(q) = -C_0 - C_1 q - C_2 \frac{q^2}{2}$
- intermittency coeffi cients $C_2 = 1.32 \pm 0.05$ $C_2 = 0.22 \pm 0.02$

Scalar 3D WTMM method: singularity spectra of galaxy distribution

Scalar 3D WTMM method:

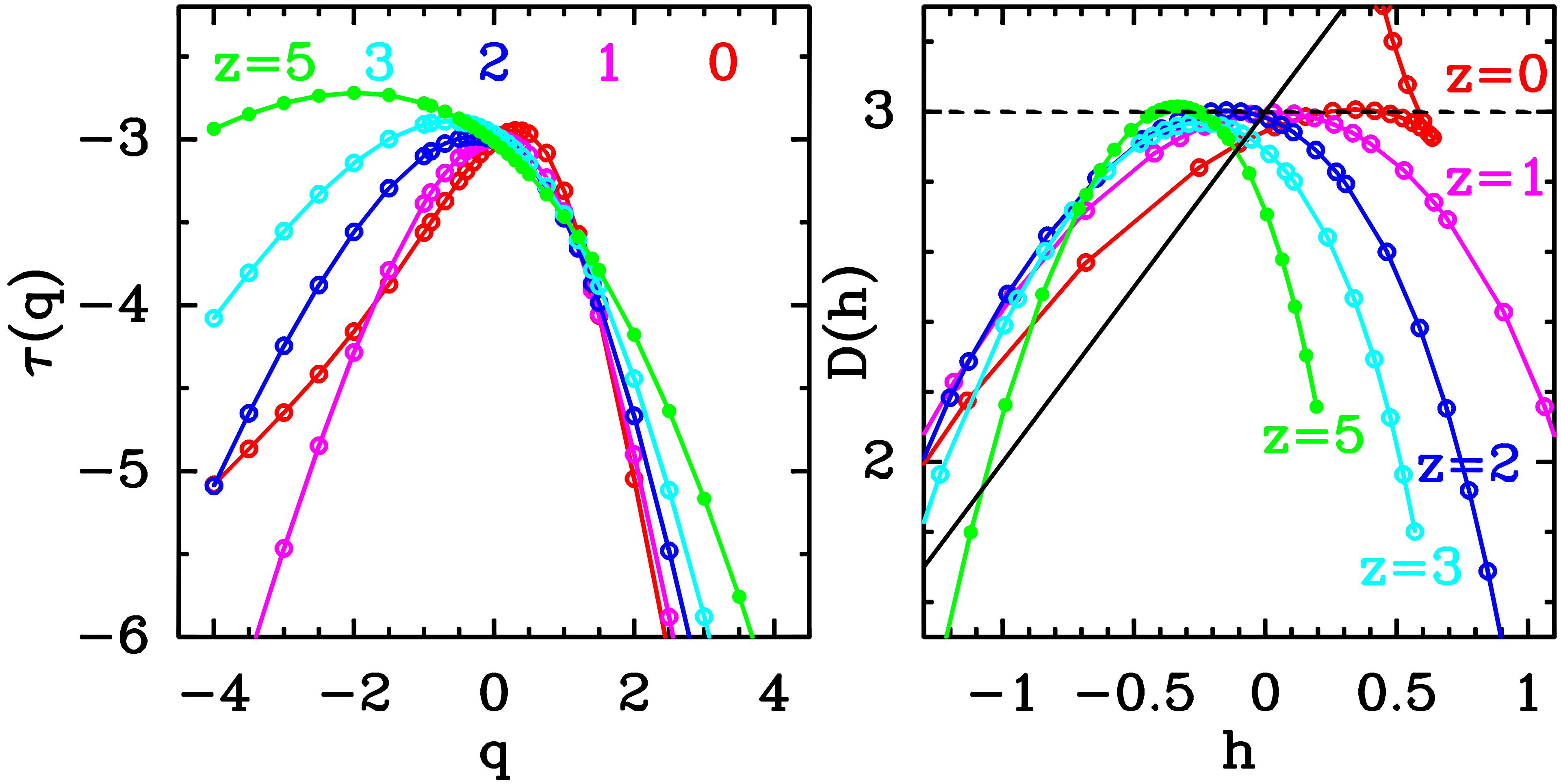

Box-Counting method: singularity spectra of galaxy distribution

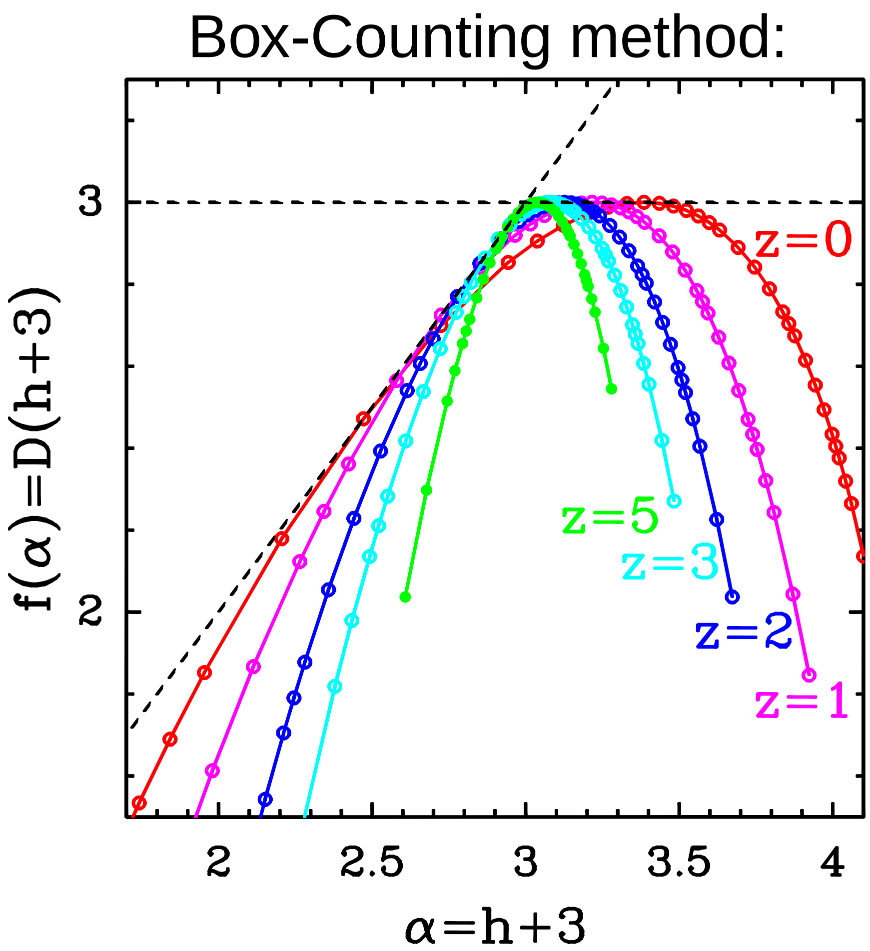

- Box-counting intermittency coefficients are smaller than those computed using 3D WTMM method !!! (To be continued).

Cancellation exponent basics

- **Signed singular measure :**
  $\forall A, \exists B \subset A / \ \mu_s(A)\mu_s(B) < 0$
  (ex : magnetic field component, ...)
- ***Cancellation exponent*** **:** $\kappa = \lim_{\varepsilon \to 0} \frac{\ln \sum_i |\mu(I_{i,\varepsilon})|}{\ln(1/\varepsilon)}$,
  where $\{I_{i,\varepsilon}\}$ **is a tiling of measure's support.**
- **using the wavelet transform:**

$$\kappa = -D_F - \tau(q = 1)$$

  $\Rightarrow$ **choice of the analyzing wavelet.**
- **link to the notion of conservativity of a multiplicative cascade:**
  $\kappa = -D_F - \tau(q = 1) = \frac{\ln < M >}{\ln b}$ **: transfert rate of the measure from scale** a **to scale** a/b
- **conservative cascade** $\Longleftrightarrow$ $\kappa = 0$
  non-conservative cascade $\Longleftrightarrow$ $\kappa \neq 0$

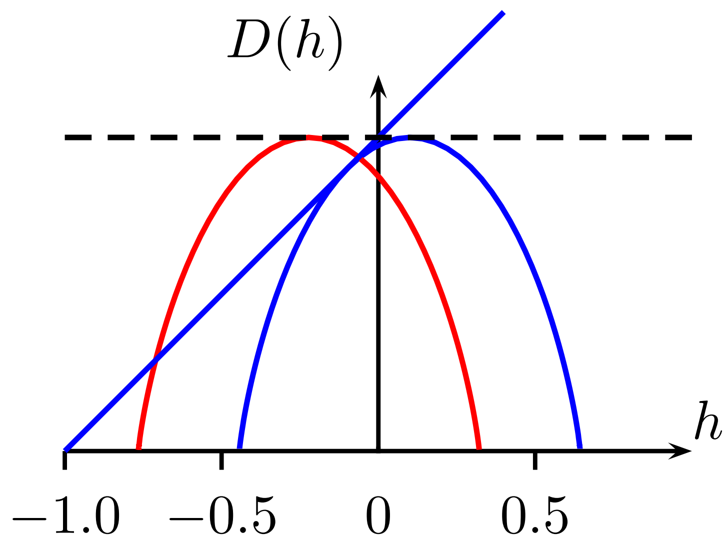

Recursive filter technics in 3D

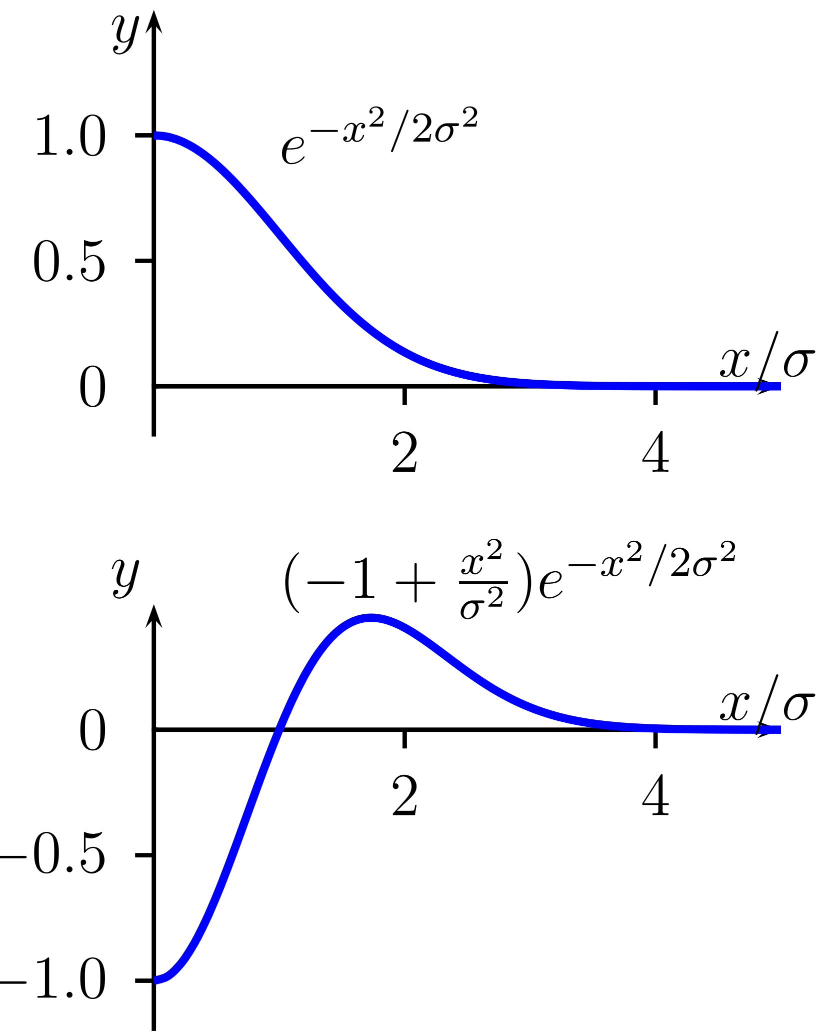

- **Gaussian filter** $e^{-x^2/2\sigma^2}$ **approximated by** $h_\sigma(x)$
  $(a_0 \cos(\omega_0 \frac{x}{\sigma}) + a_1 \sin(\omega_0 \frac{x}{\sigma})) \exp^{-b_0 \frac{x}{\sigma}}$
  $+(c_0 \cos(\omega_1 \frac{x}{\sigma}) + c_1 \sin(\omega_1 \frac{x}{\sigma})) \exp^{-b_1 \frac{x}{\sigma}}$
- **Coefficients** a_i, b_i, c_i **and** ω_i **are estimated by minimizing the relative quadratic error:**

$$\epsilon^2 = \frac{\sum_{i=1}^{10\sigma}(g_\sigma(i)-h_\sigma(i))^2}{\sum_{i=1}^{10\sigma} g_\sigma(i)^2}$$

- **4th order recursive equation:**
  $y_k = n_{00}x_k + n_{11}x_{k-1} + n_{22}x_{k-2} + n_{33}x_{k-3} - d_{11}y_{k-1} - d_{22}y_{k-2} - d_{33}y_{k-3} - d_{44}y_{k-4}$
- **computing time decrease in 3D: 60 % for Gaussian filter and 25 % for Mexican filter**

Box-counting algorithms : multifractal measure

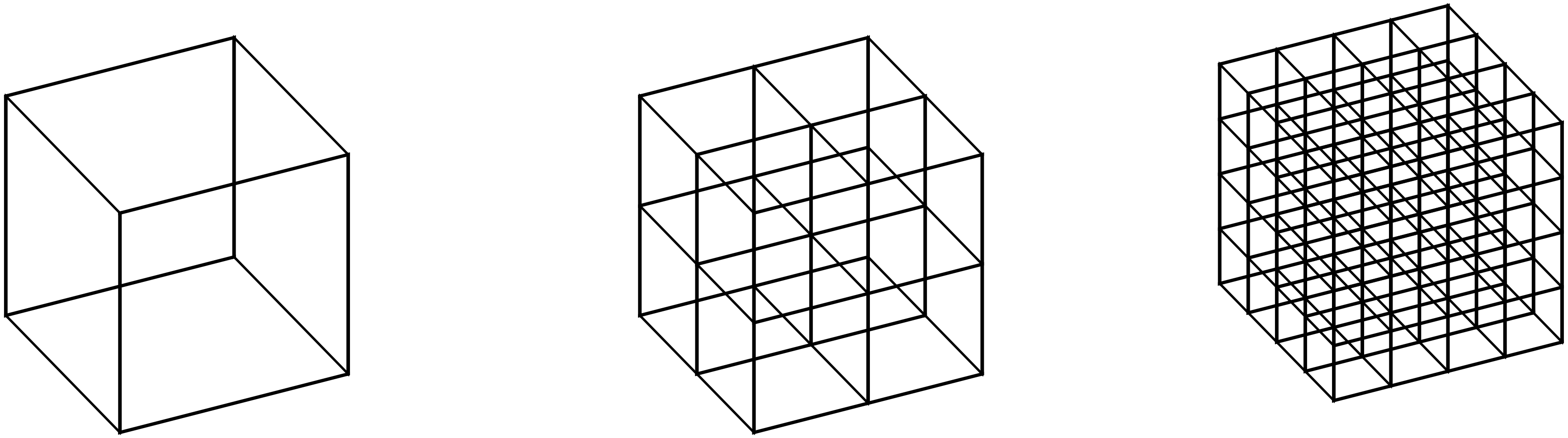

- μ: probability measure whose support $E \subset \mathbb{R}^d$
- singularity exponent: $\alpha(x) = \lim_{l \to 0} \frac{\log \mu(\mathcal{B}(l,x))}{\log l}$
- method: tile support of the measure with boxes of size $l_i = L/2^i$
- partition functions: $S_q(l_i) = \sum_{\mu(\mathcal{B}) \neq 0} [\mu(\mathcal{B})]^q = <\mu^q>$

multifractal spectrum: $\tau(q) = \lim_{l \to 0} \frac{\log S_q(l)}{\log l}$;

$$f(\alpha) = D(h = \alpha - d) = \min_q (\alpha q - dq - \tau(q))$$

Singularity spectra of velocity and vorticity

To each velocity $\mathbf{v}$ field singularity $h(\mathbf{r}_0)$ corresponds a vorticity $\omega = \nabla \wedge \mathbf{v}$ singularity $h(\mathbf{r}_0) - 1$:

$$\mathbf{f}(\mathbf{x}_0 + \mathbf{l}) = \mathbf{f}(\mathbf{x}_0) + (\nabla_{\mathbf{x}})\mathbf{f}(\mathbf{x}_0)\mathbf{l} + \ldots + (\nabla_{\mathbf{x}})^n \mathbf{f}(\mathbf{x}_0)\mathbf{l}^{(n)} + |\mathbf{l}|^{h(\mathbf{x}_0)} \mathbf{C}(\mathbf{l})$$

$$\Big\downarrow \wedge \nabla_{\mathbf{l}} \qquad \wedge \nabla_{\mathbf{l}} \qquad \wedge \nabla_{\mathbf{l}} \qquad \wedge \nabla_{\mathbf{l}}$$

$$\nabla_{\mathbf{x}} \wedge \mathbf{f}(\mathbf{x}_0 + \mathbf{l}) = \nabla_{\mathbf{x}} \wedge \mathbf{f}(\mathbf{x}_0) + \nabla_{\mathbf{x}} (\nabla_{\mathbf{x}} \wedge \mathbf{f}) (\mathbf{x}_0)\mathbf{l} + \ldots + \nabla_{\mathbf{x}}^{n-1} (\nabla_{\mathbf{x}} \wedge \mathbf{f}) (\mathbf{x}_0)\mathbf{l}^{(n-1)}$$

$$+ \quad h|l|^{h-1} \mathbf{u}_{\mathbf{l}} \wedge \mathbf{C}(\mathbf{l})$$

Goals : using WTMM method to diagnosis help of breast cancer

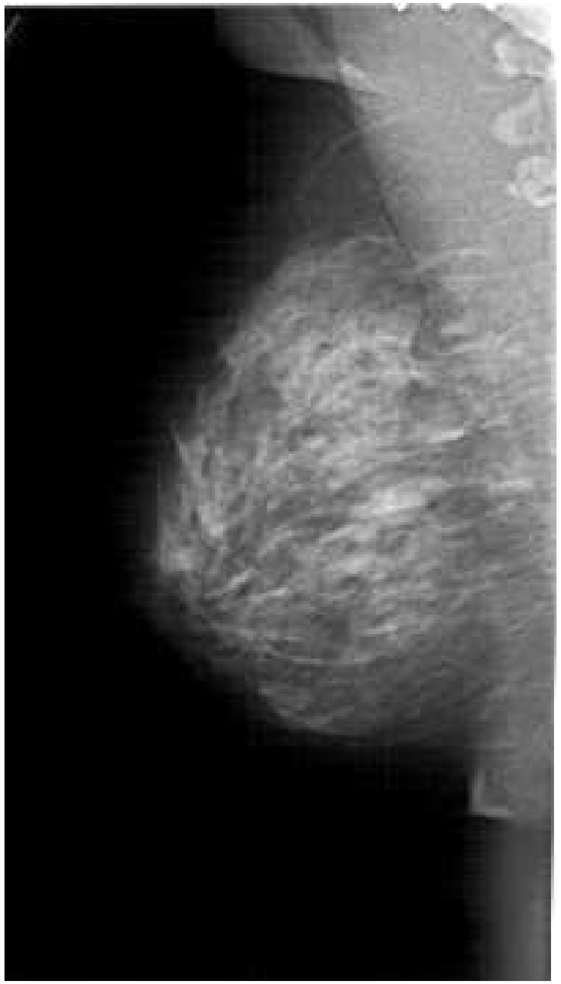

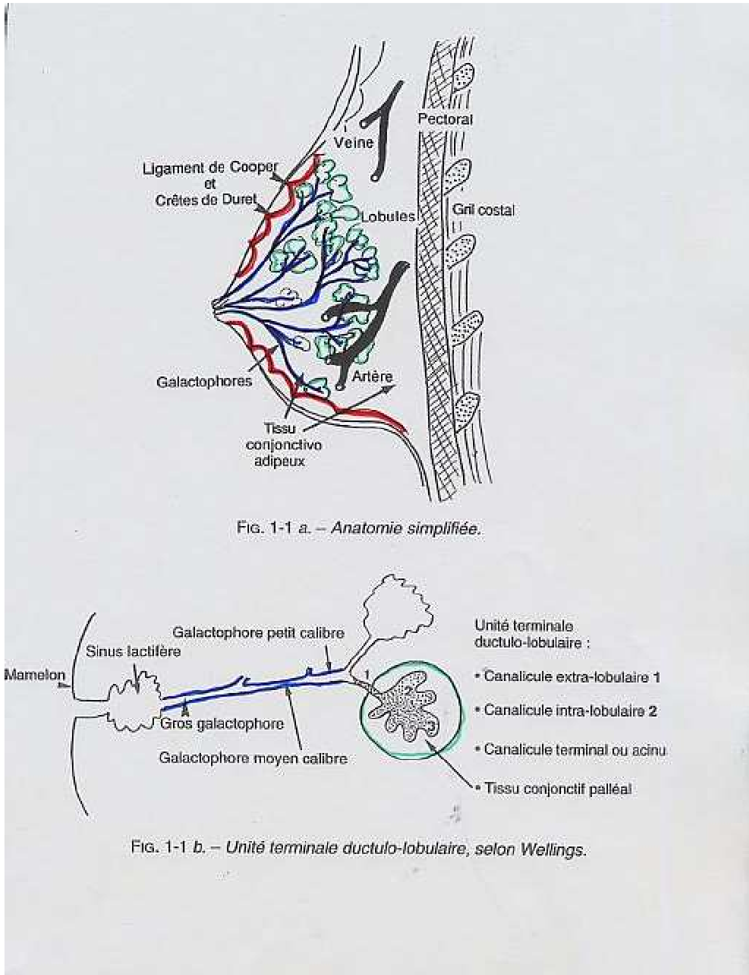

What is breast cancer ?

- malignant tumor of mammal gland
- incidence : 30000 new case each year in France
- prevention is very difficult (as opposed to lung cancer)
- hereditarity : 5 to 10 % only (BRCA1/2 genes)
- forecast depends on the tumoral volume at diagnosis

$\Rightarrow$ **SCREENING** using mammography

Radiological anomalies

- Opacities

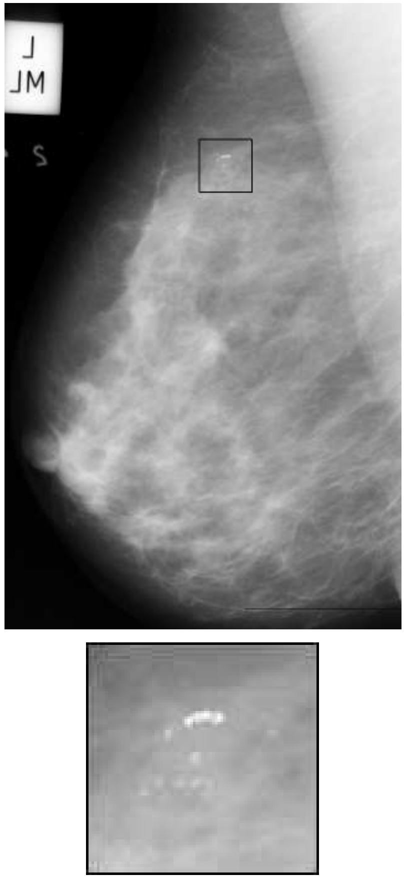

- Calcifications

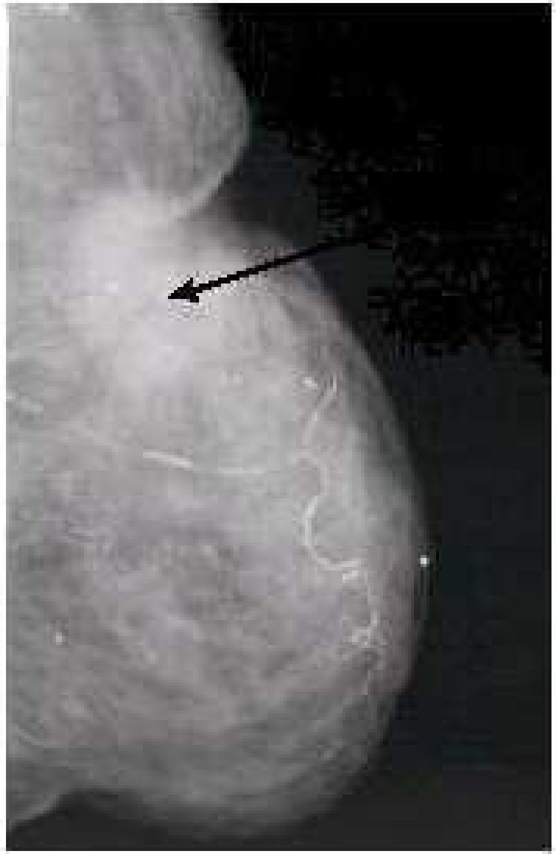

- Architectural distorcions

Digitalized mammographies : texture analysis

- dense breasts : more difficult to diagnose
- only 2 classes of monofractal properties

Digital Database for Screening Mammography:

http://marathon.csee.usf.edu/Mammography/Database.html

Dense breast

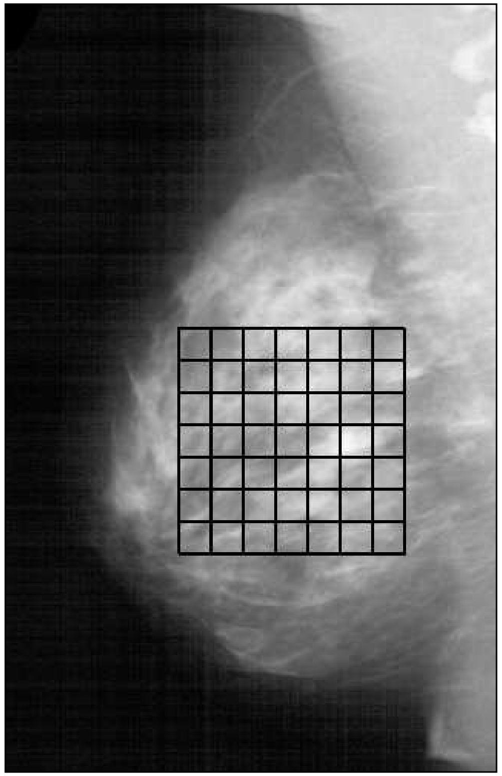

Fatty breast

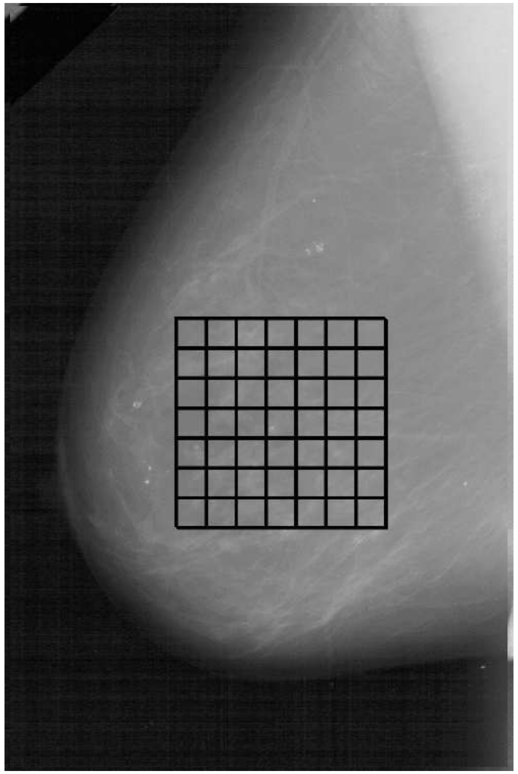

Application of 2D WTMM methodology in mammography

Tissue classifi cation : dense

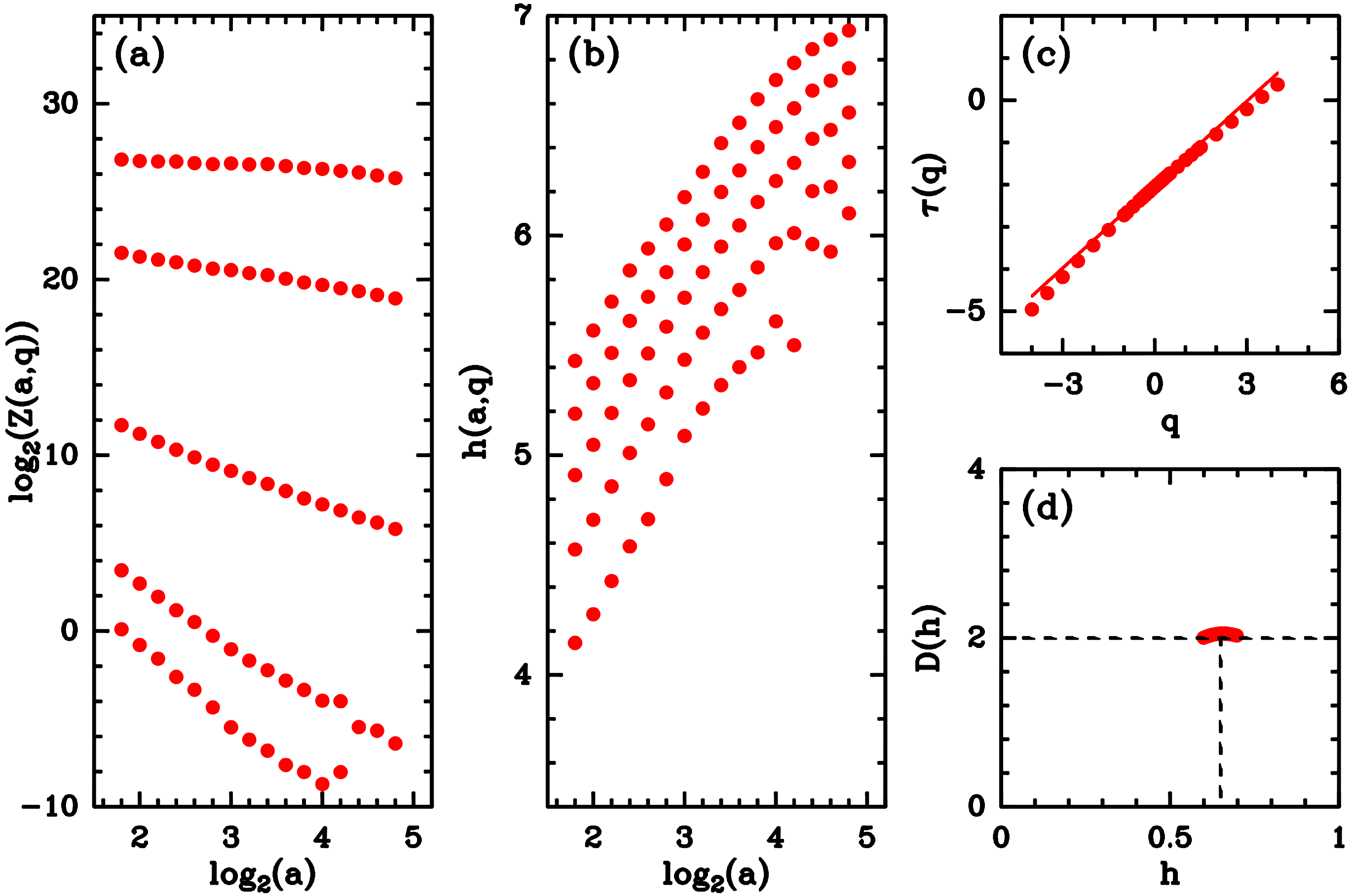

- Dense breast : monofractal, $H = 0.65$ persitent correlations

Application of 2D WTMM methodology in mammography

Tissue classification : dense vs fatty

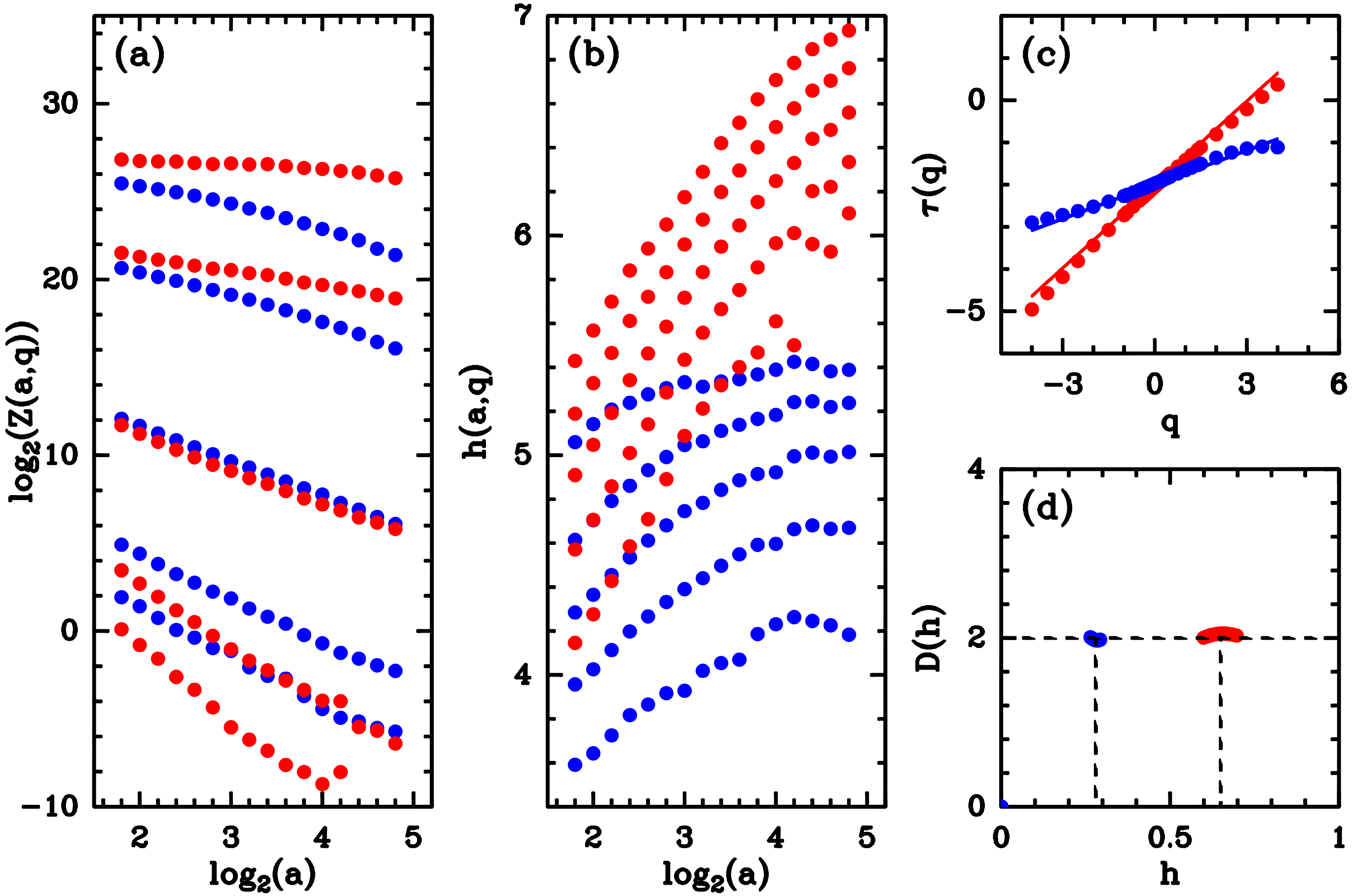

- **Dense breast :**
  monofractal, $H = 0.65$
  persitent correlations
- **Fatty breast :**
  monofractal, $H = 0.30$
  anti-persitent correlations

Application to digitalized mammographies

Colored Maps :

segmentation of dense $h > 0.52$ areas and fatty $h < 0.38$ areas

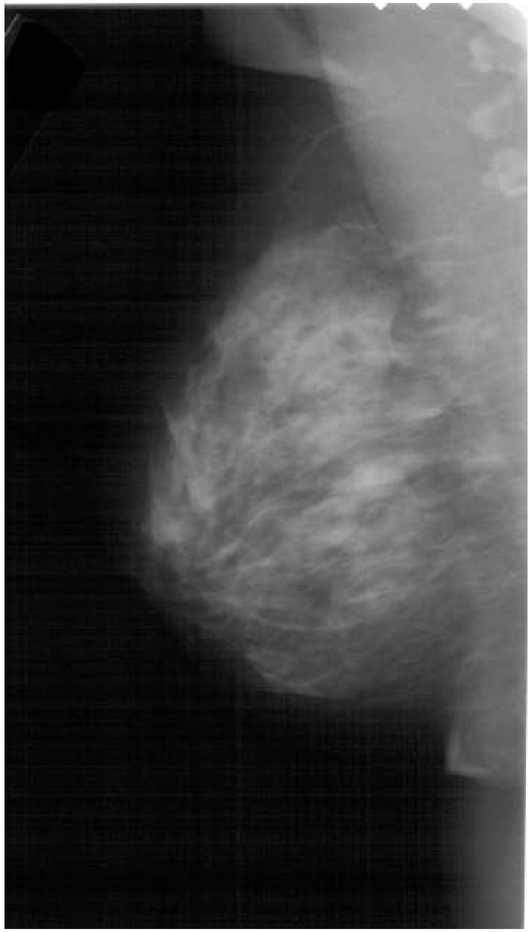

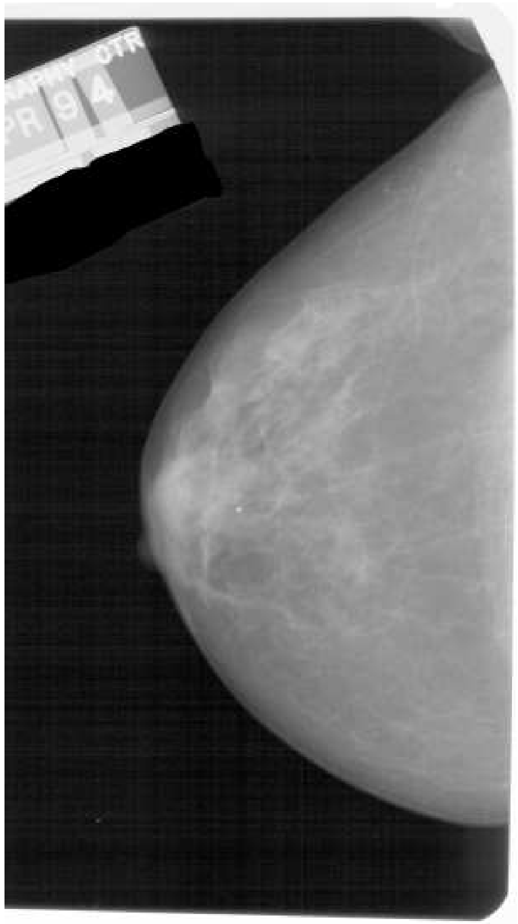

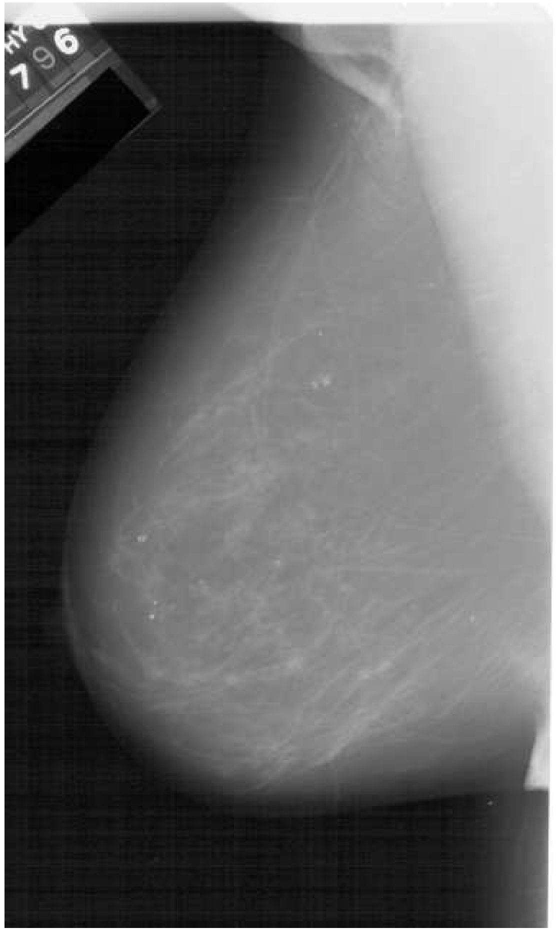

Application to digitalized mammographies

Colored Maps :
segmentation of dense $h > 0.52$ areas and fatty $h < 0.38$ areas

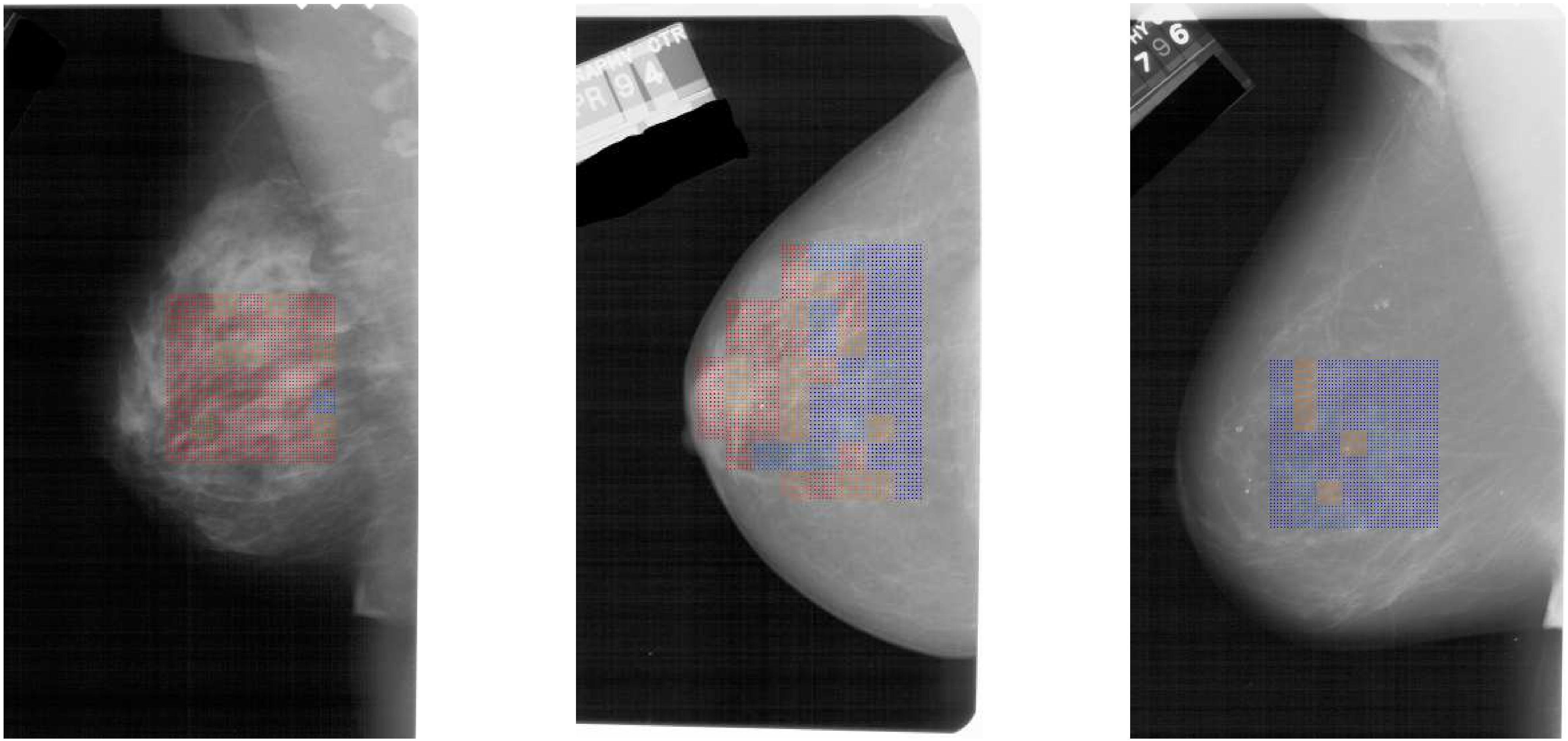

Microcalcifications detection

Segmentation of WT skeleton lines :
microcalcifications vs background texture

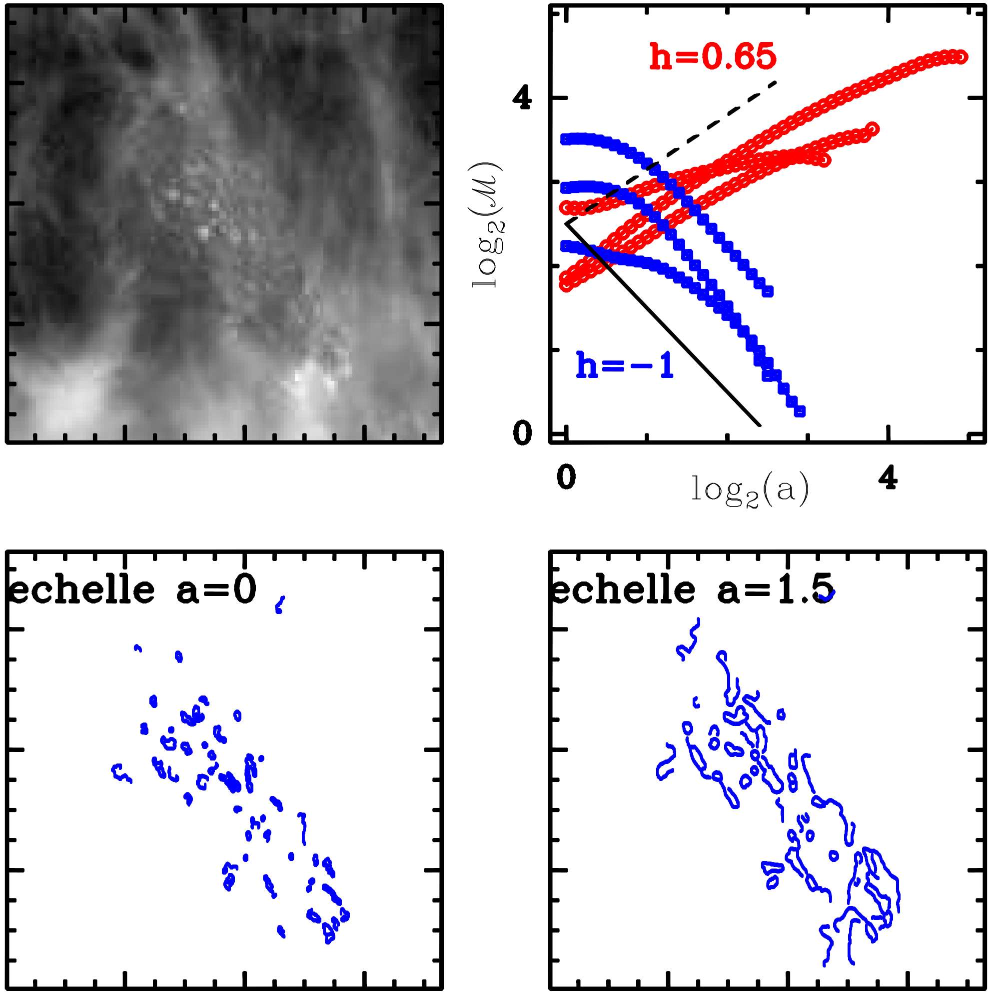

- Background lines
- Microcalcifications
  almost-punctual objects behave like 'Dirac' shapes ($h = -1$)

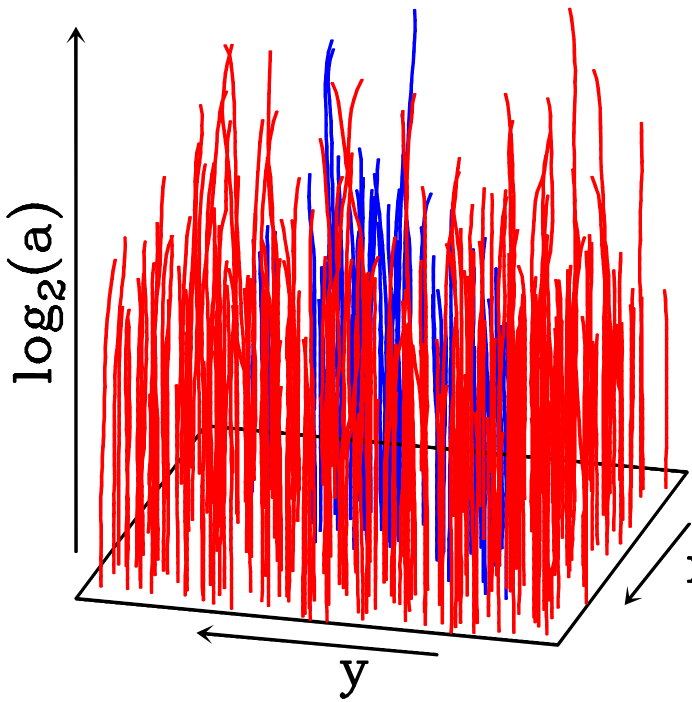

Study of microcalcification spatial distribution

Partition functions :

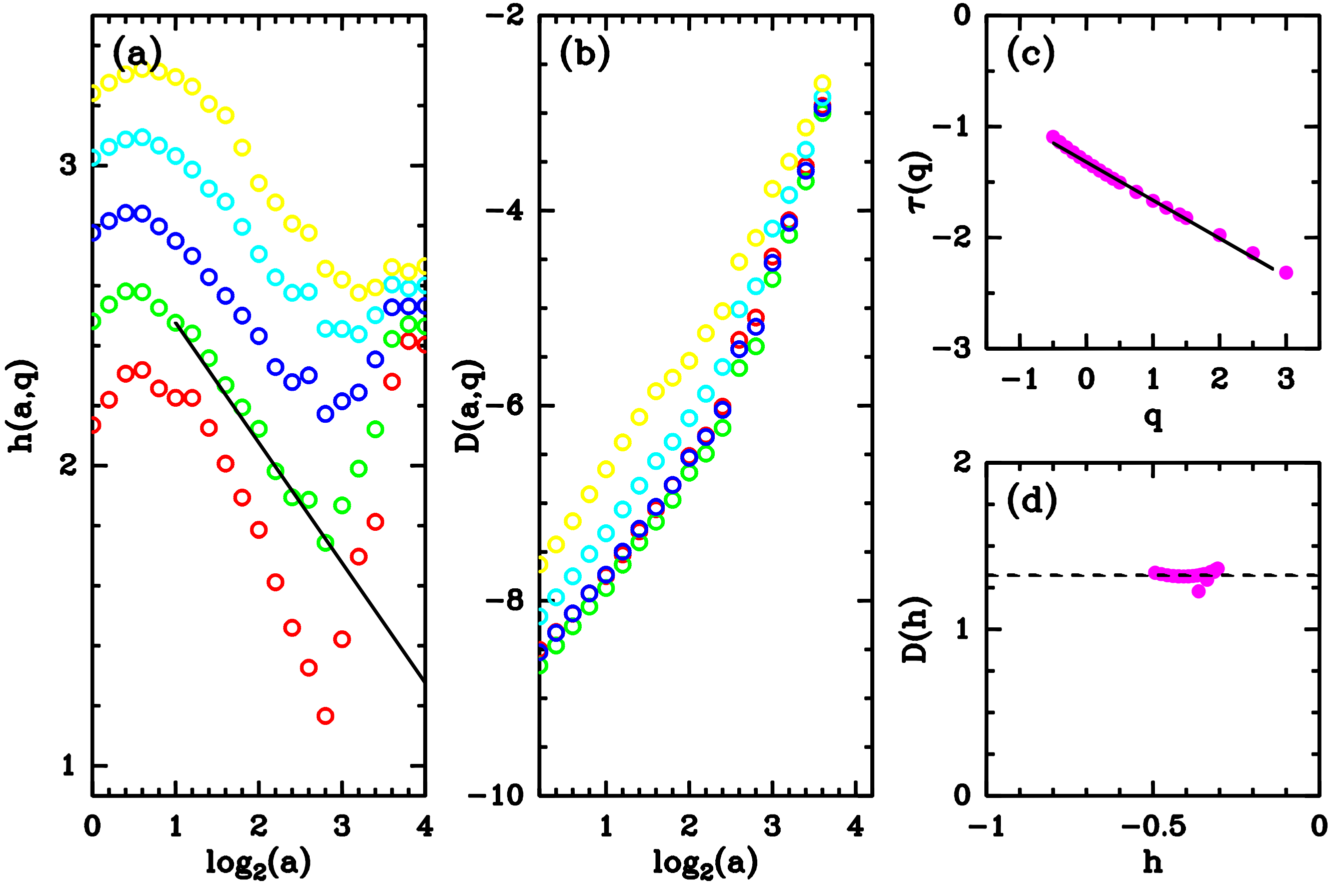

$$D_F = 1.3$$

observation :

fractal ramifi cation of cluster of microcalcifi cations $(1 < D_F < 2)$ seems to be correlated to the pathology's malignancy

Conclusions and prospects (1)

- the 2D WTMM method provides a framework for an automated measure of the breast radio-density and for studying the fractal geometry of clusters of microcalcifications.
- further study is necessary to validate quantitatively how far measuring the fractal dimension D_F could improve computer-aided diagnosis systems benign/malignant